

© [2014]This manuscript version is made available under the CC-BY-NC-ND 4.0 license <http://creativecommons.org/licenses/by-nc-nd/4.0/>
This document is the Accepted Manuscript version of a Published Work that appeared in final form in [Journal Title]. To access the final edited and published work see [<https://doi.org/10.1016/j.seares.2013.12.014>]

Relict Sand Ridges in the Continental Shelf of the Gulf of Valencia (Western Mediterranean)

Silvia Albarracín (1), Javier Alcántara-Carrió (1), Isabel Montoya-Montes (2), Ángela Fontán-Bouzas (1), Luis Somoza (3), Carl L. Amos (4) and Jorge Rey (5)
Salgado

- (1) Inst. Environmental and Marine Sciences. Universidad Católica de Valencia. Guillem de Castro 94,46001 Valencia, Spain
- (2) Dpto. de Oceanografía Física, Química e Geológica. Instituto Oceanográfico. Universidade de São Paulo. Praça do Oceanográfico 191. São Paulo, Brasil.
- (3) Instituto Geológico y Minero Español, Ríos Rosas 23, 28003 Madrid, Spain
- (4) National Oceanography Centre, University of Southampton, Southampton, UK
- (5) ESGEMAR, M5 Pier 7, Málaga port, 29001 Málaga, Spain

Abstract

The presence of fossil or relict bedforms is common in the Quaternary fill of modern continental shelf due to sea level oscillations, tectonic subsidence and migration of associated sedimentary facies. The continental margin of the Gulf of Valencia has been strongly influenced by glacio-eustasy and neotectonic. High-resolution multibeam bathymetry data, seismic reflection profiles and box core samples were collected across the continental shelf of the Gulf of Valencia during the DERIVA cruises carried out in 2010 and 2011. The integrated analysis of this data set and high-resolution mapping of the relict bedforms on the Valencian continental shelf, ranging between 50 and 90 m allowed the study of previously identified system of sand ridges located in front of the present-day Albufera de Valencia lagoon. The system is composed of 27 ridges with a NNE–SSW orientation, i.e. oblique to the present shoreline, in which the lateral horns point backwards. These sand ridges can reach 10 meters in height and 3 km in length resulting in a maximum slope of 6 degrees. According to seismic stratigraphic and relative sea level curve reconstructions, these sand ridges were formed during the Younger Dryas (≈ 10 Ky BP). Consequently, they have been classified as Holocene sand ridges associated with coastal sedimentary evolution.

Key words: Holocene, seismic stratigraphy, Continental shelf, Sand waves, Subaqueous dunes, Western Mediterranean

1. Introduction

The middle-shelf along the margin of the Gulf of Valencia is covered with a system of large linear ridges, oriented oblique to the predominant bottom current. The shelf processes generating such bedforms are influenced by steady baroclinic currents, such as intruding oceanic currents and tidal currents, and also by meteorological forcing. The seabed features of the study area vary widely in size and morphology, due to a number of different factors, such as: grain size, grain density, sediment distribution, sediment supply, and the bottom shear stress field (Amos, 1990).

Modern sedimentary processes may provide the key to understanding the conditions for the genesis of relict bedforms. The inner-shelf environment is complex as it is influenced by the interplay of the sea level stability or fluctuation and sediment transportation on not only the shelf but also the littoral. Large sand bodies preserved on the shelf can provide the main sources and deposits of sand, and can control the sand dynamics and these include barrier islands, delta lobes, large ebb-tidal deltas, shoals, ridges and other features associated with low stand river valleys.

Sand waves and large bedforms are found on continental shelves worldwide, with examples being the eastern US continental margin (Edwards et al., 2003, Fenster et al., 1990, Figueiredo et al., 1981, Goff et al., 1999, Harrison et al., 2003, McBride and Moslow, 1991, Swift et al., 1978, Twichell et al., 2003, Whitmeyer and FitzGerald, 2008), the Canadian margins (Amos and King, 1984, Amos et al., 2003, Barrie et al., 2009, Hoogendoorn and Dalrymple, 1986, Li and Amos, 1999, Piper, 1991), the Brazilian and Argentinian continental margins (Figueiredo, 1980, Parker et al., 1982), the European continental margin, in the North Sea (De Maeyer et al., 1985, Dyer and Huntley, 1999, Houboldt, 1968, Houthuys et al., 1994, Trentesaux et al., 1994, Trentesaux et al., 1999, Van de Meene et al., 1996, Van de Meene and van Rijn, 2000, Walgreen et al., 2002), those of Germany (Antia, 1994), Denmark (Anthony and Leth, 2002, Kuijpers et al., 1993) and France (Berné et al., 1998, 2007; Bassetti et al., 2006), the continental margins of India (Wagle and Veerayya, 1996), Japan (Ikehara and Kinoshita, 1994), China (Bartek and Wellner, 1995, Berne et al., 2002, Wang et al., 2012, Yang, 1989, Yoo et al., 2002), Korea (Park et al., 2003), Australia (Harris, 1988), and the margins of North and South Africa (Flemming, 1978, Flemming, 1980, Green and Smith, 2012, Ramsay et al., 1996).

Sand waves are thought to have three distinct origins: (1) sand waves that are fossil or relict features, such as barrier islands and spits which formed prior to the Holocene transgression and have only slightly been modified after their formation (e.g. Hyne and Goodell, 1967, McClennen and McMaster, 1971, McBride and Moslow, 1991). (2) Sand waves Sand waves that are still actively being formed, changing and evolving. This category typically describes Atlantic margin ridges, which are post-transgressive features and have been formed by sediment transport driven by the interaction between storm-flow and nearshore topography (Huthnance, 1982a, Huthnance, 1982b, Rine et al., 1991, Snedden et al., 1994, Swift and Field, 1981, Trowbridge, 1995). (3) Sand waves that correspond to moribund sand ridges (Liu et al., 2007).

The mechanisms responsible for the formation, mobility and stability of sand waves have been described by Boczar-Karakiewicz et al. (1990) and Trowbridge (1995). Storms and resulting infragravity wave patterns are the main agents for generating shoreface connected ridges. There are many factors to consider in the genesis and evolution of sand waves on continental shelves: (1) sea-level, before or after the Holocene transgression, which will define the ravinement surface (Bassetti et al., 2006, Berne et al., 1998); (2) dominant oceanographic processes such as tidal currents (Berné et al., 1994, Collins et al., 1995, Kenyon et al., 1981, Trentesaux et al., 1999), littoral currents (Lane and Restrepo, 2007, Whitmeyer and FitzGerald, 2008), waves (e.g. Allen, 1980, Calvette et al., 1999), dominant extreme waves in storm episodes (Berne et al., 1998, Hoogendoorn and Dalrymple, 1986, Dalrymple and Hoogendoorn, 1997, Parker et al., 1982, Snedden et al., 1994, Snedden and Dalrymple, 1999, Stubblefield and Swift, 1981, Van de Meene et al., 1996), or sediment transport

due to a combination of storms and shore currents (Figueiredo et al., 1981, Swift and Field, 1981, Swift et al., 1978, Trowbridge, 1995); (3) finally, the current stage of activity of these features (active, relict or quasi-moribund) implying that the sand waves correspond either to reworked transgressive deposits (Edwards et al., 2003, McBride and Moslow, 1991, Snedden and Dalrymple, 1999, Snedden and Dalrymple, 1999), or to post-transgressive active sand waves, which were formed via sediment transport driven by the interaction between storm-flow and nearshore topography. Several hydrodynamic mechanisms have been advanced to account for ridge formation during a period of erosional shoreface retreat. They fall into two classes: coastal boundary flow models and stability models. The two are not mutually exclusive (Figueiredo, 1980). Dyer and Huntley (1999) proposed a classification of sand ridges and banks according to their degree of evolution. Overviews of modern shelf sand ridges can be found in Snedden and Dalrymple (1999) and Snedden et al. (2011).

The environmental implications of the formation of near-shore sand waves frequently close to a lagoon and barrier, and in general oblique to them, include the presence of an inlet and mouth that contribute sediment to the system (McBride and Moslow, 1991). The recognition of such structures in the stratigraphic record may enable the reconstruction of ancient depositional environments and processes (Goff et al., 2005).

A sand wave is a composite, flow oblique (or parallel) linear accumulation of composite sand, usually of measureable relief (Amos and King, 1984). These are usually large bedforms (1–4 km wide; 2–10 km long; 2–6 m high) oriented obliquely to the regional contours (typically at 30°). Sand waves are formed in nearshore environments (e.g., Swift and Field, 1981) and, according to some authors, can continue to be modified or even entirely reformed in depths of up to 40 m (Goff et al., 1999, Rine et al., 1991, Snedden and Dalrymple, 1999, Snedden et al., 1994). However, other studies suggest that ridges become inactive in depths of over 20 m (Stubblefield and Swift, 1981, Swift et al., 1984, Stubblefield et al., 1984). At water depths such as the ones occurring in this study area, the sand waves are likely to be moribund and are most probably relict features of a shallower hydrodynamic regime (Goff et al., 1999, Swift et al., 1984).

The nearest bedforms to this study area which have been the subject of the study are located on the shelf south of the Ebro delta, near Columbretes, located at a greater depth than the ones considered here (Lo Iacono et al., 2010, Muñoz et al., 2005). Bedforms have also been reported on the continental shelf of Murcia (300 km south of Valencia), located near the coast (Fernández-Salas et al., 2013, ITGE, 1990a, ITGE, 1990b) and in the Gulf of Lion and in the Gulf of Cádiz (Berne et al., 2007, Lobo et al., 2000).

This study focuses on the interpretation of high resolution bathymetry and on the geomorphological characterization and interpretation of the seabed features of the continental shelf of the Gulf of Valencia, together with a stratigraphic sequence analysis and radiocarbon dating. This has enabled a characterization to be made of the environmental conditions prevailing during the formation of these sand waves and their evolution up to the present day..

2. Regional setting

2.1. Morphotectonic setting

The continental shelf of the Gulf of Valencia (Western Mediterranean) is located from 38.9° to 40° N and from 0.5° W to 0.5° E, with a total length of ca. 111 km (Fig. 1). The continental margin of the Gulf of Valencia is bounded landward by the Eastern Iberian Range and seaward by the Valencia Trough. It extends from Sagunto in the north to La Nao Cape in the south, with structures following a NE–SW trend parallel to the regional Neogene Betic alignment (Acosta et al., 2013, Maillard and Mauffret, 2012).

The continental shelf of the Gulf of Valencia represents the transition between the passive continental Ebro margin in the north, with an intense progradation, and the Betic continental margin in the south, controlled by neotectonic activity. The Valencia Basin represents an aborted rift being linked to the Oligo-Miocene opening of the Northwestern Mediterranean basin in a back-arc context (Maillard and Mauffret, 2012).

The main morphological characteristic of this continental shelf is its very variable width, ranging from 275 km in the north to 68 km in the south. The inner and a part of the outer shelf are characterized by a great variety of sedimentary morphologies and environments, which are greatly influenced by continental factors (Maldonado and Zamarreño, 1983, Rey and Fumanal, 1996, Rey et al., 1999). However, the middle shelf presents the sea bottom subhorizontal with slightly seaward slope and erosive forms which are evidence of a great morphological complexity (Díaz del Río V and Fernández-Salas LM, 2005, Díaz del Río et al., 1986, Maldonado et al., 1983).

Before the Holocene, sand supplied by rivers accumulated on the inner shelf seaward of the present shoreline, but the sedimentary contribution of the rivers in the region has changed since then. In the past, the Júcar and Turia rivers provided larger sediment loads during wet periods. The basal fluvial sediments are composed of Early Holocene or Pleistocene deposits from the Turia River, associated with a very distant coastline (Carmona, 1995). In the present day, the influence of the continental sediment supply from the Ebro River primarily affects the northern sector of the Gulf of Valencia (Alvárez et al., 2010).

Evidence of sea level eustatic oscillation in conjunction with a high rate of local subsidence in the region has been provided by numerous authors (Blázquez et al., 1996, Díaz del Río et al., 1986, Fumanal et al., 1993, Goy and Zazo, 1973, Goy et al., 1996, Rey and Díaz del Río, 1983, Rey and Fumanal, 1996, Viñals and Fumanal, 1995, Zazo et al., 1993). Morphological evidence of sea level changes has been identified, such as cemented beach deposits at a depth of 50 m in the southern margin of the Gulf of Valencia (Fumanal et al., 1993, Viñals, 1995, Viñals and Fumanal, 1995), associated to isotopic stage 5e (112,000–119,000 y BP), and, more recently, Pleistocene paleobarrriers with associated paleo-lagoon deposits have been located in the sedimentary record of the continental shelf (Albarracin et al., 2013). The most modern of these deposits have been found as outcrops on the inner shelf and are associated with the isotopic stage 5e (Alcántara-Carrió et al., 2013). Moreover, two remarkable paleochannels eroded over the most modern barrier have been associated with isotopic stage 2 (Alcántara-Carrió et al., 2013).

Small fluctuations of the sea level rise in the Mediterranean during the Holocene are reflected in beach and barrier systems, deltas such as that of the Ebro (Somoza et al., 1998), and the Albufera

lagoon (the central sector of the present coast of the Gulf of Valencia). Thus, during the mid to late Holocene the marine transgression deposits suggest that the Albufera lagoon was not totally open to the sea (Marco-Barbas, 2010) and the system had a different hydrographic network than that of the present day. Evidence of this past hydrographic network includes the identified paleochannels and the inlet submerged at a depth of 25–30 m offshore from the Albufera lagoon (Albarracín et al., 2009, Alcántara-Carrió et al., 2013).

Sand waves were discovered in the Gulf of Valencia in the 1980s (Díaz del Río et al., 1986, Giró and Maldonado, 1983, Maldonado and Zamarreño, 1983, Maldonado et al., 1983, Rey and Díaz Del Río, 1982, Rey and Díaz del Río, 1983, Rey and Díaz del Río, 1984, Rey and Medialdea, 1989, Young et al., 1983) and they were recognized as relict and currently subject to storm events.

2.2. Seismicity

The area south of Valencia and Alicante is one of the most seismically active areas in the Iberian Peninsula, with mainly shallow earthquakes and the main orientation being ENE–WSW (Alfaro et al., 2002, Silva et al., 2003).

The Gulf of Valencia can be considered a seismic gap (silent area) showing very few events, and these being of the lowest magnitudes and intensities. Nevertheless, in the past, destructive earthquakes have been recorded: in 1396, an earthquake (Ms 6.5) destroyed the town of Tavernes de la Valldigna, Valencia (Giner et al., 2003). The seismic activity is associated with the eastern margin of the Betic Internal Zone (Alfaro et al., 2002). About 90% of the events have depths of less than 9–11 km, with most being moderate events, having magnitudes of less than 4.0 Mb.

Other seismically active locations are associated with rift structures shown in the accumulation of earthquakes in Fig. 2. Tectonic evidence and sedimentary evidence of the Mediterranean rifting episode are well preserved in the continental margins of the Gulf of Valencia (Renault et al., 1984, Silva et al., 2003). Some epicenters show a clear relationship with active offshore structures such as the western prolongation of the Valencia Trough. The event whose focal mechanism is shown in Fig. 2, had a magnitude of 4.2 Mb and a depth of 10 km, and can be explained in terms of a possible NE–SW trending plane, compatible with the fault trends displayed in the area (De Vicente et al., 2008, Olaiz et al., 2009, Rueda and Mezcuca, 2005).

In the Gulf of Valencia, several dextral strike-slip faults have a broad NE–SW to NNE–SSW orientation sub-parallel to the coast, coinciding with the general direction of the inland coastal mountain alignments and separated by intermediate valleys (graben type) which approximately coincide with northern Catalanides structures. This lineament corresponds to distensive phases contemporaneous with the Balearic basin formation, as coastal depressions developed to the south forming a seaward listric fault system, which gradually depressed the reliefs of the Iberian Range (NW–SE) in the north and reached the Betic Range (ENE–WSW) in the south. The Albufera lagoon is a possible focus of subsidence in the Betic direction toward the Valencia Trough, as shown by the alignment of earthquakes in this direction. The Albufera lagoon area where the earthquakes are located, shows relatively low Vf (Valley floor/width ratio) values (0.65–0.70) (Silva et al., 2003) and also shows continuous subsidence from Late-Pleistocene to Holocene (Zazo et al., 1993).

2.3. Oceanographic Setting

Large-scale circulation in the Northwestern Mediterranean Sea is relatively constant due to the distribution of the water bodies in the region. These are in dynamic equilibrium, generating a cyclonic thermohaline circulation (Font et al., 1986). On the continental shelf the general circulation is easily altered by the influence of local winds and the effects of continental discharges, resulting in much more variable circulation patterns.

Circulation on the Mediterranean shelf is largely driven by wind even in areas influenced by freshwater inputs (Estournel et al., 2003, Jordà and De Mey, 2010). The absence of significant tides (micro-tidal regimen, $TR < 0.3$ m) reinforces the importance of wind forcing in the coastal and shelf regions of the Gulf of Valencia (Jordi et al., 2011).

The database analysis of wave predictions obtained by the WAM (Wave Prediction Model, WAMDI Group, 1988), e.g. at point 2083111WANA (0.08° W 39.25° N) demonstrated that the dominance of NE and SE components of the storm wave regime was seen, with storm wave regime of $H_s > 5$ m and associated T_p ranging between 9 and 14 s (Fig. 3). In addition, the analysis of the REDEXT Buoy II (2630) data (0.21° E, 39.52° N), recorded by Puertos del Estado (www.puertos.es), shows the predominance of bidirectional currents (Fig. 3b).

3. Materials and methods

The study area is located 15 km seaward of the present sand barrier offshore of the La Albufera lagoon (Fig. 1, Fig. 4). It covers 100 km² of the continental shelf ranging from 50 to 90 m in depth (Fig. 4). Three geophysical surveys took place in this region over a three year period (2009–2011): in July 2009 aboard the R/V Isla de Alborán; in September 2010 aboard the R/V Garcia Del Cid; and in July 2011 aboard the R/V Sarmiento de Gamboa. During these cruises, equipment including shallow-water multibeam echosounders, subbottom profilers (such as the 3.5 kHz, Chirp and TOPAS systems) and medium-to-high resolution seismic systems (such as GeoPulse). GPS data for navigation and location of the geophysical data in all these surveys were processed using Hypack software.

Multibeam echosounder data were collected in the central Valencia Gulf in water of between 50 and 90 m in depth (Fig. 4) in September 2010 aboard the RV Garcia del Cid (DERIVA and COSTEM projects) using a Seabeam 1050D (ELAC NAUTIK) system operating at a frequency of 180 kHz. Sound velocities were calibrated by means of CTD profiles. The raw multibeam data were processed with the CARIS® software to obtain a digital bathymetric model (DBM) with a 5×5 m grid resolution. Spatial analyses of the multibeam data were performed using the ArcGIS® software to obtain a comprehensive regional digital elevation model (DEM). The total set of bathymetric data was then processed using Arc GIS® for the interpretation and generation of 2D and 3D environments that enabled the geomorphological characteristics (slope, orientation, drainage systems) of the study area to be deduced.

A HASP box-corer was used to take surface sediment samples along the whole area of the Gulf of Valencia in 2009 aboard the R/V Isla de Alborán. One of these sediment samples was located in the study area. Grain size analysis and weight percentage of carbonates were determined for each centimeter in depth of this sample, up to a total depth of 20 cm. Grain size analysis was carried out using a Coulter LS 230 in the Instituto de Ciencias del Mar (CSIC), and grain size distribution was calculated with the GRADISTAT software (Blott and Pye, 2001) to obtain a Folk diagram for sedimentary classification (Folk, 1954). Carbonate content (% CaCO₃) was determined with a Bernard calcimeter.

The stratigraphic record of the continental shelf in the Gulf of Valencia was obtained by means of a geophysical survey drawing on different seismic techniques (Fig. 4). 9.8 km of seismic records were taken using a 3.5 kHz mud penetrator, with a 100 ms recording interval, aboard the Isla de Alborán vessel in July 2009. Additional 6.5 and 5 km seismic profiles parallel to the coast were recorded aboard the R/V Garcia del Cid in September 2010 using a Boomer GeoPulse 205J, with a 200–2000 Hz frequency and resolution ranging from 0.3 to 0.4 m, which enables recognizable sequences to be obtained from 30 to 100 m in sediment depth. The Boomer data were acquired using the Sonar Wiz.SBP v.2.79 (Chesapeake—Geoacoustics) software and processed with Sonar Wiz.map (Chesapeake) software.

In July 2011, aboard the R/V Sarmiento de Gamboa, 4 ultra-high resolution TOPAS (Atlas Parasound P-35) seismic reflection profiles were recorded, which were 3.8, 2, 4.5 and 6.5 km in length and with typical recorded depths of being up to 66 m (Fig. 10). The TOPAS profiles were acquired with a Chirp wavelet, operating at two simultaneous frequencies. Ultra-high resolution profiles obtained from Chirp, which operates at a primary high frequency (PHF) of 15.5 kHz and secondary lower frequency (SLF) of 0.75 kHz using the parametric effect in the water, allowed us to obtain a maximum vertical resolution of 6 cm. Data were acquired and processed with the PARASTORE software.

Finally, 3.5 kHz seismic profiles collected by the R/V Garcia Del Cid in 1983 (database of the Instituto de Ciencias del Mar, CSIC) were reanalyzed (Fig. 4). These geophysical data consist of 25 km long seismic profiles, taken perpendicular to the coast (Maldonado et al., 1983) as part of a joint Spanish–United States project studying the Valencia shelf.

4. Results

4.1. Morphological Features

The DEM of the studied area on the Valencia middle continental shelf covers about 64 km², an area more than 6.5 km wide and approximately 11 km long (Fig. 4, Fig. 5). This reveals the presence of 24 linear bedforms (19 prominent ridges, labeled D1 to D19, and 5 mounds, labeled M1 to M5), at a water depth ranging from 53 to 80 m (Fig. 5). Three additional bedforms (D20 to D22), not recorded in the multibeam data, were identified and mapped with seismic profiles at the south-eastern limit of the study area.

The dimensions of these bedforms, given in Table 1, show that they have variable axial lengths, ranging from 679 m (M4) up to 3404 m (D3). The maximum width of about 216 m is very similar in all of the bedforms. The maximum height ranges from 1.5 to 8.5 m (Table 1). In summary, these bedforms correspond to a total volume of sand of about 50 million m³. The wavelength between bedforms ranges from 443 m (D1–M3) to 1791 m (D17–D19). On average the slope along the continental shelf in the study area is from 0.5° to 1°. Stoss slopes on the bedforms are gentle, with an average slope of 1.2° and a maximum of 2°, while lee faces range from 0.5° to maximum values of 6° (D9), with average values ranging from 3 to 4°. The mounds show lower angles in their both stoss and lee faces. The topographic profiles show that the top of the bedforms is quite horizontal, with average slopes of 1° (Fig. 6).

These bedforms are grouped in ten parallel lines with a NNE–SSW orientation with the lateral horns pointing backwards, which allow us to define them as longitudinal 2d dunes with some asymmetry, similar to parabolic dunes. This orientation is 61° clockwise from the modern shoreline and 41° clockwise from the stronger currents in the area, which run N–S (Font et al., 1990).

These sand waves are large bedform features which are of ~ 10 m height, ~ 1.5 km wide and up to 10 km in length, therefore they correspond to very large, flow-transverse, 2D subaqueous dunes according to the terminology in Ashley (1990). These sand waves in the Gulf of Valencia are higher and have larger wavelengths than those in other study areas (Fig. 7).

4.2. Grain size analysis

Analysis of the grain size of a box core sample taken at 80 m depth, close to the bedforms, enabled the top 20 cm of the sediments to be characterized and they were found to be composed of poorly sorted sandy silt (Fig. 8).

There was a noteworthy presence in some sub-samples of rounded, slightly fattened, quartz gravels, ranging from 5 to 15 mm in size (8b and 8c), which were not significant in weight (< 2%), and yet also clearly indicative of a nearshore depositional environment. The carbonate content ranges from 50% up to 60% (ave. 55%), with the principal remaining minerals being quartz and clays (illite and kaolinite).

4.3. Seismic stratigraphy

The combination of three different seismic techniques (GeoPulse, TOPAS and 3.5 kHz) over the same area provides different resolutions, different penetrations and therefore complementary information on the seismic stratigraphy. GeoPulse profiles enabled the description of deep seismic units to take place, while the TOPAS system ensured that high resolution (cm scale resolution) profiles from the superficial units below the bedforms could be obtained and finally, the 3.5 kHz profiles facilitated the determination of the internal structure of the bedforms. The reanalysis of a 3.5 kHz profile acquired in 1983 enabled the large-scale identification of different seismic units.

In Fig. 9, an example of a high resolution GeoPulse profile is shown together with the DEM, both with a vertical exaggeration of $10 \times$ (Fig. 9). This seismic profile enabled the identification of seismic units of coarse deposits, a seismic unit of marine fine deposits and another more surficial seismic unit of sand waves. The following seismic units can be identified on the GeoPulse seismic profile, from the bottom to the top:

1 — The Upper Pleistocene regressive wedge, with two regressive subsystems: FRW1 and FRW2. These subsystems are 20 to 60 m thick, display an internal structure with linear reflectors, are non-chaotic and show a downlap base. The FRW2 subunit is topped by a transgressive erosional surface of high reflectivity (T1) located at 35–40 m in depth. The transgressive system tract (TST) starts in the transgressive subsystem St1 with a transgressive erosional surface (T1) and then continues with progradational marine unit (P1), which corresponds to coarse Pleistocene shelf deposits, slightly tilted (low gradient), 30–35 m deep, 20 m thick. It presents coarse sediments on the bottom (T1) and on the top (T2). The transgressive erosional surface is represented by a notably irregular reflector (T2), with clinoforms appearing at a depth of 10–20 m and with coarse deposits which are not well defined using this seismic technique (Fig. 9). The transgressive subsystem (St2) starts with an aggradational unit (A2), characterized by linear and regular reflectors followed by a progradational unit (P2) with more irregular and tilted reflectors, 10 m thick. The top of this progradational unit is characterized by an irregular erosional surface composed of gravel deposits, which corresponds to the ravinement surface (RS). The sediment sample described in Fig. 8 corresponds to the outcrop of this gravel deposit, combined with modern mud.

The formation of this ravinement surface (RS) is associated with a fast transgressive phase, with subsequent sediment reworking. The sand ridge unit (SU) is characterized, in section, by a mounded shape with oblique and regular internal reflectors.

The spatial analysis of the sub-superficial seismic units was also carried out by means of the interpretation of four topographic parametric sounder (TOPAS) profiles, parallel to the coast (Fig. 10). This high resolution but lower penetration technique enables images to be obtained of the seismic unit beneath SU and T2, but it does not permit the identification of the deeper Pleistocene coarse deposits. The seismic units found in each profile from coast to shelf, can be described as follows. At the bottom of profile 1 coarse irregular deposits (T2) with an irregular surface and several mound like structures can be observed. This unit is topped by an aggradational deposit that is part of the transgressive subsystem (St2). Sand waves deposited over the high reflectivity RS are interpreted as a surface with coarse granulometry. In profile 2, the T2 deposits are characterized by stepped mounds and irregular reflectors with different characteristics on the southward side. RS appears as coarse deposits outcropping on the surface and its origin is associated either with the influence of the coast or with differential erosion. Bedforms (SU) D18 and D20, mapped using seismic techniques are flanked by coarse deposits with irregular RS reflectors, forming a wedge that finishes in contact with T2. The changes to the lateral facies can be explained by the southern influence of the mouth of the Jucar River which has eroded the modern sediments.

The T2 surface is characterized with a dark reflector corresponding to coarse deposits, which are discontinuous and stepped in profile 3. This constitutes an erosive surface with variable morphology

(channels, fluvial–marine system) without ruling out the occurrence of wave ravinement erosion formation processes. Aggradational deposits above T2 correspond to the transgressive subsystem (St2). The sand waves unit (SU) corresponds to coarse sediments on the lee slope, at the inner part of each sand ridge.

In the deepest profile 4, the sand waves D19 and D22 which are well defined as continuous seismic units are shown, but between the two ridges the reflectors are much more irregular from the surface to 5 m in depth (D22). This is interpreted as corresponding to an outcropping hard surface with high reflectivity.

Four seismic units are identified on the seismic profile GC83 across the continental shelf (Fig. 11). The older seismic unit is characterized by high acoustic impedance and irregular reflectors, corresponding to the Pleistocene coastal barrier system (PB) from the Tyrrhenian, as reported in Albarracín et al. (2013). At deeper locations across the shelf, it is possible to identify a transgressive surface (T2), with irregular reflectors, corresponding to an erosive surface with coarse sediments. Continual, regular and horizontal reflectors are part of the transgressive subsystem (St2). In the middle part of the profile it is possible to identify two sub-superficial bedforms: the SU, most probably composed of alternating medium–fine and coarse sediments. The thickness of these SU bedforms ranges from 5 to 10 m. Beneath the RS, a Holocene gravel deposit is observed. Relict slump deposits (SLU) are located in the talus below the RS surface. In this profile, the most noteworthy feature is that SU is a relict unit situated above PB and therefore these deposits are not contemporaneous.

The sub-bottom profiler enabled the identification of the bedforms' internal structure (Fig. 12). These bedforms have fossilized over the basal graveled Holocene surface that corresponds to the RS unit, before the development of the SU. Sand waves are classified as relict because a vertical accretion can be observed, demonstrating that at present they do not suffer any lateral movements. Finally, the facies of fine sediments of the present-day continental shelf are characterized by high reflectivity and parallel and regular acoustic reflectors. The older continental shelf deposits are covered by these fine Holocene deposits (H), which are a few meters in thickness, although they become thinner (< 1 cm) as one moves eastwards.

5. Discussion

5. 1. Late Quaternary stratigraphic evolution

The clusters of earthquakes in the Gulf of Valencia are associated with faults, which are parallel and transverse to the coast (Fig. 2) and point to the neotectonic reactivation of the basement faults within a distensive regime (Díaz del Río et al., 1986, Goy and Zazo, 1988, Goy et al., 1996) affecting the Neogene–Quaternary deposits. This neotectonic activity is also shown by the presence of slumps at the outer edge of the continental shelf (Acosta and Herranz, 1983), as observed on the eastern edge of one of the seismic profile (Fig. 11).

There are subsidence depressions where marshes and small lagoons have been developed (Rey and Fumanal, 1996). Other evidence of subsidence is the Pleistocene alluvial deposits that were

superimposed by the river Turia, because of the continued subsidence of the plain (Sanjaume and Carmona, 1995). Moreover, evidence of a sustained high rate of Holocene subsidence can be seen in the presence on the continental shelf at 20 m in water depth of organic sediments with freshwater swamp facies (~ 10,000 ky BP) in a core sample taken at the southern coastline of the Gulf of Valencia, indicating that the shoreline was much further out than it is today (Viñals et al., 1993). A high degree of subsidence (8–21 cm/ky, with an average value of 12.8 cm/ky) has been reported by Zazo et al. (1993) but other authors report even higher figures of up to 45 cm/ky of subsidence in the south of the study area (Rey and Fumanal, 1996). We propose that the Pleistocene coastal barrier system opposite of the Albufera lagoon was formed during the prolonged Tyrrhenian (120 ky ago) sea-level highstand. This indurated Pleistocene coastal barrier is located at 30 m in water depth in the central part of the Gulf of Valencia (Albarracín et al., 2013, Alcántara-Carrió et al., 2013). This would entail a subsidence rate of 30 cm/ky in the central region of the Gulf of Valencia (Fig. 13). By taking into consideration the regional neotectonics and local subsidence, a curve of relative sea level changes in the Gulf of Valencia has thus been deduced (Fig. 2).

The transgressive deposits, composed of several retrogradational parasequences, underlay this transgressive erosional surface (ravinement surface) and are stacked vertically in the sectors nearest to the inner shelf (Hernández-Molina et al., 1994). Therefore, the ravinement surface represents the Younger Dryas erosive event and constitutes the base on which the sand waves settle (Fig. 10, Fig. 2). Similarly, most of the sediment accumulated on the inner and middle shelves of the Rhône corresponds to transgressive deposits. This fact denies the hypothesis of the last deglacial sea level rise, which was too fast to allow the deposition of large sediment bodies on the shelf (Berné et al., 2007). The transgressive deposits laid down above the wave ravinement surface derive from shoreface erosion and/or from longshore drift. They are usually very thin, but thicken where the transgression was punctuated by regressive pulses or where offshore sand ridges form (Cattaneo and Steel, 2003).

The formation of the sand waves occurred in less than 1000 years, between 9 and 10 ky BP (Fig. 2, light blue period), corresponding to relative sea level being – 50 m of the present day, as the sand ridge field is located in water ranging between 55 and 80 m in depth. The coastal hydrodynamics favored the formation of these larger bedforms. According to their morphological characteristics, without internal bedding structures, they are interpreted as coastal sand waves. Similar bedforms can be found in South Carolina (Denny et al., 2013) and on the inner shelf off west-central Florida in the Gulf of Mexico (Edwards et al., 2003, Harrison et al., 2003).

The time relationships of large-scale coastal sand bodies, such as beach ridges or large-scale bar-trough systems and shore-connected sand bodies, are of the order of 101–102 years after the onset of stable forcing conditions (Cowell et al., 1999).

Two sources of sediment supply to the sand waves can be suggested: i) the reworking of deposits associated with the transgressive surface (Cattaneo and Steel, 2003) and ii) the downstream sediment supply from the river inlet located in front of the Albufera lagoon, i.e. NW of the sand waves. With regard to the first hypothesis, the absence of cross-bedding in the sand waves could indicate that lateral migration did not occur, with the sand waves being formed instead of individual coastal bars. This hypothesis is supported by the presence of a plateau of marsh or swamp, due to the low slope

of the shelf. Thus, the reworking of the ravinement surface on its own would supply the coarse material for the construction of the sand waves, as well as the irregular initial topography of the basement surface (Edwards et al., 2003 and Harrison et al., 2003). The river sediment supply could be related to fluvial inputs across local inlets eroded over the indurated Pleistocene sand barrier (Alcántara-Carrió et al., 2013). The presence of coarse sediments in the sediment sample analyzed could be indicative of the vicinity of a fluvial system.

5.2. Mechanism of formation of the sand ridges

The sand waves of the Gulf of Valencia are relict bedforms that, according to the seismic profiles recorded, are composed of coarse materials and are located in situ, without significant migration from their formation location. The age of formation of these sand waves is associated with the Younger Dryas i.e. with a sea level located 30 to 50 m below the present-day sea level.

A tidal origin for the sand waves in the Mediterranean area can be ruled out, since there is only a microtidal regime. Two mechanisms can be proposed for the morphogenetic formation of the sand waves, which are not necessarily incompatible: (i) the influence of storm waves and (ii) longshore littoral drift (Fig. 14).

Lateral redistribution processes induced by storm flow activity favors the seaward transport of coarse sediments and the generation of bedforms on the inner shelf of the Gulf of Valencia (Giró and Maldonado, 1983, Young et al., 1983). The present-day wave regime shows the presence of high storm waves with $H_s > 5$ m and T_p ranging between 9 and 14 s (Fig. 3) which correspond to wave base levels of 63 to 150 m respectively. This means that even storm waves with the present-day sea level can affect the sand ridge field, eroding their surface and the thin layer of fine sediments covering them. Nevertheless, the storm-built sand ridge topography in the Gulf of Valencia is no longer active since it is presently mantled by several decimeters of early Holocene mud (Maldonado et al., 1983).

The lower sea level of 10 ky ago, at the time of the formation of the sand waves enabled greater interaction of storm waves with the sand ridge deposits (Fig. 14). Similarly, a lower sea level implies that the bedforms would have been located in shallower water and consequently they would also be strongly affected by the longshore littoral drift. The crest orientation of the sand waves and the backward orientation of their horns are coherent with the presence of longshore currents to the south-east, related to either normal waves or more likely storm wave events.

5.3. Comparison of the sand ridges in the western Mediterranean: The last sea level rise

The continental margin of the Gulf of Valencia has been strongly influenced by glacio-eustatic changes and by tectonics, as has the entire western margin of the Mediterranean Sea (Stocchi and Spada, 2009). During the Last Glacial Maximum, 22 ky ago, the sea level in the Valencia region was at -110 m, compensated by the hydro-isostatic effect (Lambeck and Bard, 2000). The marine

transgression during the glacial to interglacial transition between 18 and 8 ky reworked the outer shelf as the high energy nearshore zone retreated (Gardner et al., 1990). The superficial sediment infill of the continental shelf of the Gulf of Valencia corresponds to a Quaternary depositional sequence, attributed to transgressive deposits. In contrast, during the Holocene, the marine transgression caused the coastline to migrate inland, with the consequent destruction of previous coastal morphologies (Rey and Fumanal, 1996). The stillstand period at about 10.5 ky BP is associated with the Younger Dryas climatic event (Somoza et al., 1998).

In the Northwestern Mediterranean the presence of bedforms corresponds to ancient transgressive sand deposits over the last 20 ky BP, following Bassetti et al. (2006). The same authors described the sand bodies formed during the last post-glacial transgression, along the edge of the shelf of the Gulf of Lion, as transgressive fossil ridges, lying over a major erosive surface. They probably formed during the Younger Dryas (15–12 ky BP), during a period of deceleration of the rise in sea-level that was long enough to favor the formation of these sedimentary bodies.

The Rhône deltaic system of the Gulf of Lion displays aggradation, starting at ~ 15 ky BP, followed by progradation initiated during the first phase of the Younger Dryas. Clinofolds with ages ranging between ~ 11,100 and ~ 10,600 y BP, are above the coarse lag of the ravinement surface (~ 15 ky BP). The time-frame encompasses the end of the Bølling–Allerød, the Younger Dryas and the Preboreal (Berné et al., 2004, Berne et al., 2007).

Bedforms on the Maresme continental shelf (NE Iberian margin, north of Barcelona) are found in different steps according to the eustatic curve of Aloise (1986): the deepest sand body (95–113 m) was active during the initial stages of sea level rise about 15 ky BP, the second body (35–80 m) was built up during a continuous transgressive rise after a stillstand or short regressive period, at about 8–10 ky BP, and finally the shallowest sand body (15–30 m) formed at about 6 kyBP (Díaz and Maldonado, 1990).

The sand waves located at 70 m in water depth on the Ebro continental shelf are interpreted as relict sand facies associated with shoreline (Díaz et al. 1990). Thus, their formation was associated with reworking and downdrift transport of late Pleistocene shelf-margin delta sandy deposits laid down during periods of deceleration during the last transgressive phase, which have been dated, by means of shell fragments, as being 11,100 yBP (Díaz et al., 1990).

In the southern margin of the Ebro continental shelf, near the Columbretes Islands, two groups of large subaqueous dunes at 60 and between 80 and 116 m water depth, are presumably younger than 13 (Muñoz et al., 2005) and 11 ky BP (Lo Iacono et al., 2010), respectively.

Near Águilas, on the outer continental shelf in Murcia (south of Valencia), sand waves were found at between 65 and 105 m in water depth, with an oblique orientation in relation to the current shoreline. There are considered to be relict deposits, possibly not only formed during the last transgressive period but also influenced by the present-day current hydrodynamic regime whose direction is predominantly northeastward (Acosta et al., 2013, Fernández-Salas et al., 2013, ITGE, 1990a, ITGE, 1990b).

6. Conclusions

The combined analysis of the detailed bathymetry, the seismic units, the grain size analysis of seafloor sediments and the regional oceanographic and climatic regimes enabled us to establish a relative sea-level curve and to identify the most probable scenario for the formation of the sand waves on the continental shelf of the Gulf of Valencia (Fig. 10):

1.

A total of 27 sand waves have been identified in the central region of the Gulf of Valencia continental shelf. They cover an area of at least 65 km² and are located in ten parallel lines with a NNE–SSW orientation. The morphology of these bedforms corresponds to subaqueous dunes with mound ridges and pointing backward horns. The presence of coarse sediments indicates that the origin of these sedimentary deposits is associated with a nearshore environment.

2.

The seismic stratigraphy of the central region of the Gulf of Valencia is characterized by an Upper Pleistocene forced regressive wedge (stages FRW1, FRW2) and by transgressive systems (stages St1 to St3). Stage St2 is composed of a transgressive surface (T2), aggradational deposits (A2) and progradational deposits (P2). Over P2, the base of the sand waves corresponds to a ravinement surface (RS) which defines the morphology underlying the later formation of the sand ridge units (SUs).

3.

Taking into consideration the regional neotectonics and local subsidence, a subsidence rate of 30 cm/ky has been calculated for the central region of the Gulf of Valencia, and applied to the reconstruction of the relative sea level curve during the last 120 kyBP.

4.

According to these seismic stratigraphic and relative sea level curve reconstructions, the sand waves were formed during the Younger Dryas (~12-10 kyBP) with the sea level located 30 to 50 m below the present-day sea level.

5.

The origin of these sand waves is associated with coastal sedimentary processes: Two compatible formation mechanisms can be proposed: (i) the sand waves were formed by the influence of storm waves and (ii) the sand waves are the result of longshore littoral drift. The lateral redistribution processes induced by storm flow activity favor the seaward transport of coarse sediments and the generation of bedforms of this type. Nevertheless, a lower sea level also entails that these bedforms would be located in shallower water, and consequently, they would be strongly affected by the longshore littoral drift. The sand waves are currently relict, although even with the present-day sea-level, extreme storm waves can affect the sand ridge field, eroding the thin layer of fine modern sediments covering their surface.

Acknowledgments

The authors are indebted to all the participants of the DERIVA oceanographic cruise aboard the “García del Cid” and “Sarmiento de Gamboa” research vessels. This research is a contribution to the CTM2009-09479 and ACOPLAT projects. It has been partially supported by the complementary CTM2010-09488-E, CTM2010-11032-E, and ACOMP/2011/257 projects. We would like to thank Dr. Victor Diaz Del Rio from the Instituto Español de Oceanografía and Dr. Marcel.li Farran

from the Instituto de Ciencias del Mar (CSIC) for providing us with digitized seismic profiles from their historical database (GANSA'82 and GC'83).

As well we are indebted to Dr. Pere Puig, Dr. Jorge Guillem, Marta Ribo and COSTEM Project (Ref: CTM2009-07806) for providing us part of multibeam data used, was collected during a COSTEM-2, cruise from 17-23 September 2010.

References

- Acosta, J., Herranz, P., 1983. Morfología y tectónica de la plataforma continental, entre Gandía y Sagunto (Golfo de Valencia). IV Asamblea Nacional de Geodesia y Geofísica 3, 1303–1323.
- Acosta, J., Fontán, A., Muñoz, A., Muñoz-Martín, A., Rivera, J., Uchupi, E., 2013. The morpho-tectonic setting of the Southeast margin of Iberia and the adjacent oceanic Algero-Balearic Basin. *Marine and Petroleum Geology* 45, 17–41.
- Albarracín, S., Alcántara-Carrió, J., Montoya, I., Sánchez, M.J., Rey, J., Blázquez, A., 2009. Análisis morfológico de la plataforma continental del Golfo de Valencia: la antigua desembocadura fluvial de la Albufera de Valencia. In: Cuban National Oceanographic Committee, Latin American Association of Marine Sciences (Eds.), *Proceedings of the 8th Latino-American Congress of Marine Sciences*, Havana, Cuba, p. 1210.
- Albarracín, S., Alcántara-Carrió, J., Barranco, A., Sánchez García, M.J., Fontán Bouzas, Á., Rey Salgado, J., 2013. Seismic evidence for the preservation of several stacked Pleistocene coastal barrier/lagoon systems on the Gulf of Valencia continental shelf (western Mediterranean). *Geo-Mar. Lett.* 33 (2–3), 209–216.
- Alcántara-Carrió, J., Albarracín, S., Montoya Montes, I., Flor-Blanco, G., Fontán-Bouzas, A., Rey Salgado, J., 2013. An indurated Pleistocene coastal barrier on the inner shelf of the Gulf of Valencia (western Mediterranean): evidence for a prolonged relative sea-level stillstand. *Geo-Mar. Lett.* 33 (2–3), 217–224.
- Alfaro, P., Delgado, J., Estévez, A., Soria, J.M., Yébenes, A., 2002. Onshore and offshore compressional tectonics in the eastern Bétic Cordillera (SE Spain). *Mar. Geol.* 186, 337–349.
- Allen, J.R.L., 1980. Large transverse bedforms and the character of boundary-layers in shallow-water environments. *Sedimentology* 27 (3), 317–323.
- Álvarez, C., Amore, O., Cros, L., Alonso, B., Alcántara-Carrió, J., 2010. Coccolithophore biogeography in the Mediterranean Iberian Margin. *Rev. Esp. Micropaleontol.* 42 (3), 359–371.
- Aloïsi, J.C., 1986. Sur un modèle de sédimentation deltaïque: contribution à la connaissance des marges passives. Unpublished Doctoral Thesis, University of Perpignan 162.
- Amos, C.L., 1990. Modern sedimentary processes. In: Keen, M.J., Williams, G.L. (Eds.), *Geology of the Continental Margin of Eastern Canada*. Geological Survey of Canada, *Geology of Canada*, 2, pp. 609–673 (also *Geological Society of America, The Geology of North America*, vol. I-10029).
- Amos, C.L., King, E.C., 1984. Bedforms of the Canadian eastern seaboard; a comparison with global occurrences. *Mar. Geol.* 57, 167–208.
- Amos, C.L., Li, M.Z., Chiocci, F.L., La Monica, G.B., Cappucci, S., King, E.H., Corbani, F., 2003. Origin of shore-normal channels from the shoreface of Sable Island, Canada. *J. Geophys. Res. Oceans Atmos.* 108, 1–16.
- Anthony, D., Leth, J.O., 2002. Large-scale bedforms, sediment distribution and sand mobility in the eastern North Sea off the Danish west coast. *Mar. Geol.* 182, 247–263.
- Antia, E.E., 1994. Vertical patterns of grain-size parameters of shoreface-connected ridges in the German bight. *Geol. Mijnb.* 73 (1), 13–22.
- Ashley, G.M., 1990. Classification of large-scale subaqueous bedforms; a new look at an old problem. *J. Sediment. Res.* 60, 160–172.
- Barrie, J.V., Conway, K.W., Picard, K., Greene, H.G., 2009. Large-scale sedimentary bedforms and sediment dynamics on a glaciated tectonic continental shelf: examples from the Pacific margin of Canada. *Cont. Shelf Res.* 29 (5–6), 796–806.
- Bartek, L.R., Wellner, R.W., 1995. Do equilibrium conditions exist during sediment transport studies on continental margins — an example from the East China Sea. *Geo-Mar. Lett.* 15 (1), 23–29.
- Bassetti, M.A., Jouet, G., Dufois, F., Berné, S., Rabineau, M., Taviani, M., 2006. Sand bodies at the shelf edge in the Gulf of Lions (Western Mediterranean): deglacial history and modern processes. *Mar. Geol.* 234, 93–109.
- Berné, S., Trentesaux, A., Stolk, A., Missiaen, T., De Batist, M., 1994. Architecture and longterm evolution of a tidal sandbank: the Middelkerke Bank, Southern North Sea. *Mar. Geol.* 121, 57–72.
- Berné, S., Lericolais, G., Marsset, T., Bourillet, J., de Batist, M., 1998. Erosional offshore sand ridges and lowstand shorefaces: examples from tide- and wave-dominated environments of France. *J. Sediment. Res.* 68, 540–555.

- Berné, S., Vagner, P., Guichard, F., Lericolais, G., Liu, Z.X., Trentesaux, A., Yin, P., Yi, H.I., 2002. Pleistocene forced regressions and tidal sand ridges in the East China Sea. *Mar. Geol.* 188 (3–4), 293–315.
- Berné, S., Rabineau, M., Flores, J.A., Sierro, F.J., 2004. The impact of Quaternary Global Changes on Strata Formation. Exploration of the shelf edge in the Northwest Mediterranean Sea. *Oceanography* 17, 92–103.
- Berné, S., Jouet, G., Bassetti, M., Dennielou, B., Taviani, M., 2007. Late Glacial to Preboreal sea-level rise recorded by the Rhône deltaic system (NW Mediterranean). *Mar. Geol.* 245, 65–88.
- Blázquez, A.M., Fumanal, M.P., Olmo, J., 1996. Rasgos sedimentológicos de la plataforma interna valenciana (tramo Oliva-la Vila Joiosa) y su relación con la geomorfología continental. *Cad. Lab. Xeolóxico Laxe* 21, 671–683.
- Blott, S.J., Pye, K., 2001. GRADISTAT: a grain size distribution and statistics package for the analysis of unconsolidated sediments. *Earth Surf. Process. Landforms* 26, 1237–1248.
- Boczar-Karakiewicz, B., Amos, C.L., Drapeau, G., 1990. The origin and stability of sand ridges on Sable Island Bank. *Scotian Shelf. Cont. Shelf Res.* 10, 683–704.
- Calvette, D., Falques, A., Deswart, H.E., Dodd, N., 1999. Non-linear modeling of shoreface-connected sand ridges. In: Kraus, N.C., McDougal, W.G. (Eds.), *Coastal Sediments '99*. Am. Soc. Civil Eng., 2, pp. 1123–1138.
- Cattaneo, A., Steel, R.J., 2003. Transgressive deposits: a review of their variability. *Earth Sci. Rev.* 62 (3–4), 187–228.
- Carmona, P., 1995. Análisis geomorfológico de abanicos aluviales y procesos de desbordamiento en el litoral de Valencia. *Cuad. de Geogr.* 57, 17–34.
- Collins, M.B., Shimwell, S.J., Gao, S., Powell, H., Hewitson, C., Taylor, J.A., 1995. Water and sediment movement in the vicinity of linear banks: the Norfolk Banks, southern North Sea. *Mar. Geol.* 123, 125–142.
- Dalrymple, R.W., Hoogendoorn, E.L., 1997. Erosion and deposition on migrating shoreface-attached ridges, Sable Island, Eastern Canada. *Geoscience Canada* 24 (1), 25–36.
- Cowell, P.J., Hanslow, D.J., Meleo, J.F., 1999. The Shoreface. In: Short, A.D. (Ed.), *Handbook of Beach and Shoreface Morphodynamics*. John Wiley, New York.
- De Maeyer, P., Wartel, S., De Moor, G., 1985. Internal Structures of the Nieuwpoort bank (Southern North Sea) Netherlands. *Journal of Sea Research* 19 (1), 15–18.
- De Vicente, G., Cloetingh, S., Muñoz-Martín, A., Olaiz, A., Stich, D., Vegas, R., Galindo-Zaldívar, J., Fernández-Lozano, J., 2008. *Tectonics* 27, 1–22.
- Denny, J.F., Schwab, W.C., Baldwin, W.E., Barnhardt, W.A., Gayes, P.T., Morton, R.A., Warner, J.C., Driscoll, N.W., Voulgaris, G., 2013. Holocene sediment distribution on the inner continental shelf of northeastern South Carolina: implications for the regional sediment budget. *Cont. Shelf Res.* 56 (2013), 56–70.
- Díaz del Río V., Fernández-Salas L.M. (2005). El margen continental Del Levante Español y las Islas Baleares. In: Martín Serrano A (ed) *Mapa geomorfológico de España y del margen continental 1:1.000.000*. Madrid, pp 177–188.
- Díaz del Río, V., Rey, J., Vegas, R., 1986. The Gulf of Valencia continental shelf: extensional tectonics in Neogene and Quaternary sediments. *Mar. Geol.* 73, 169–179.
- Díaz, J., Maldonado, A., 1990. Transgressive sand bodies on the Maresme continental shelf, western Mediterranean Sea. *Mar. Geol.* 91, 53–72.
- Díaz, J.I., Nelson, C.H., Barber, J.H., Giró, S., 1990. Late Pleistocene and Holocene sedimentary facies on the Ebro continental shelf. In: Nelson, C.H., Maldonado, A. (Eds.), *The Ebro Margin*. *Mar. Geol.* 95, pp. 333–352.
- Dyer, K.R., Huntley, D.A., 1999. The origin, classification and modelling of sand banks and ridges. *Cont. Shelf Res.* 19, 1285–1330.
- Edwards, J.H., Harrison, S.E., Locker, S.D., Hine, A.C., Twichell, D.C., 2003. Stratigraphic framework of sediment-starved sand ridges on a mixed siliciclastic/carbonate inner shelf, west-central Florida. *Mar. Geol.* 200, 195–217.
- Estournel, C., Durrieu de Madron, X., Marsaleix, P., Auclair, F., Julliard, C., Vehil, R., 2003. Observation and modelisation of the winter coastal oceanic circulation in the Gulf of Lions under wind conditions influenced by the continental orography (FETCH experiment). *J. Geophys. Res.* 108 (C3), 8059.
- Fenster, M.S., Fitzgerald, D.M., Bohlen, W.F., Lewis, R.S., Baldwin, C.T., 1990. Stability of giant sand waves in eastern Long Island Sound, U.S.A. *Mar. Geol.* 91, 207–225.
- Fernández-Salas, L.M., Bruque, G., DíazdelRío, V., López-Rodríguez, F.J., Vázquez, J.T., 2013. Análisis de alta resolución de un campo de ondulaciones submarinas en la plataforma externa frente a Águilas (Murcia, SE España). *Geo-Temas* 14, 175–178.

- Figueiredo, A.G.D., 1980. Response of water column to strong wind forcing, southern Brazilian inner shelf: implications for sand ridge formation. *Mar. Geol.* 35, 367–376.
- Figueiredo, A.G.D., Swift, D.J.P., Stubbleeld, W.L., Clarke, T.L., 1981. Sand ridges on the inner Atlantic shelf of North America: morphometric comparisons with Huthnance stability model. *Geo-Mar. Lett.* 1, 187–191.
- Flemming, B.W., 1978. Underwater sand dunes along southeast African continental margin — observations and implications. *Mar. Geol.* 26, 177–198.
- Flemming, B.W., 1980. Sand transport and bedform patterns on the continental-shelf between Durban and Port Elizabeth (southeast African continental-margin). *Sediment. Geol.* 26, 179–205.
- Flemming, B.W., 1988. Zur klassifikation subaquatischer, strömungstransversaler transportkörper. *Bochum. Geol. Geotechn. Arb.* 29, 44–47.
- Folk, R.L., 1954. The distinction between grain size and mineral composition in sedimentary-rock nomenclature. *J. Geol.* 62, 344–359.
- Font, J., Juliá, A., Rovira, J., Salat, J., Sánchez-Pardo, J., 1986. Circulación marina en la plataforma continental del Ebro determinada a partir de la distribución de masas de agua y los microcontaminantes orgánicos en el sedimento. *Acta Geol. Hisp.* 21–22, 483–489.
- Font, J., Salat, J., Juliá, A., 1990. Marine circulation along the Ebro continental margin. *Mar. Geol.* 95, 165–177.
- Fumanal, M.P., Mateu, G., Rey, J., Somoza, L., Viñals, M.J., 1993. Las Unidades morfosedimentarias cuaternarias del litoral del Cap de la Nau (Valencia-Alicante) y su correlación con la plataforma continental. In: Fumanal, M.P., Bernabeu, J. (Eds.), *Estudios sobre Cuaternario. Medios Sedimentarios, Cambios Ambientales, Hábitat Humano*. Universidad de Valencia, Valencia, pp. 53–64.
- Gardner, J.V., Dean, W.E., Alonso, B., 1990. Inorganic geochemistry of surface sediments of the Ebro shelf and slope, northwestern Mediterranean. *Marine Geology* 95 (3–4), 225–245.
- Gardner, J.V., Dartnell, P., Mayer, L.A., Hughes Clarke, J.E., Calder, B.R., Duffy, G., 2005. Shelf-edge deltas and drowned barrier island complexes in the Northwest Florida outer continental shelf. *Geomorphology* 64, 133–166.
- Gardner, J.V., Calder, B.R., Hughes Clarke, J.E., Mayer, L.A., Elston, G., Rzhonov, Y., 2007. Drowned shelf-edge deltas, barrier islands and related features along the outer continental shelf north of the head of De Soto Canyon, NE Gulf of Mexico. *Geomorphology* 89, 370–390.
- Giner, J.J., Molina, S., Jáuregui, P.J., 2003. Sismicidad en la Comunidad Valenciana (C.V.). *Física de la Tierra* 15, 163–187.
- Giró, S., Maldonado, A., 1983. Definición de facies y procesos sedimentarios en la plataforma continental de Valencia (Mediterráneo occidental). In: Castellví, J. (Ed.), *Estudio oceanográfico de la plataforma continental Española*. Sem Interdisc Hispanic-American Cooperative Research Project. Gráficas Buper, Barcelona, pp. 75–96.
- Goff, J.A., Swift, D.J.P., Duncan, C.S., Mayer, L.A., Hughes-Clarke, J., 1999. High-resolution swath sonar investigation of sand ridge, dune and ribbon morphology in the offshore environment of the New Jersey margin. *Mar. Geol.* 161, 307–337.
- Goff, J.A., Austin, J.A., Gulick, J.S., Nordfjord, S., Christensen, B., Sommerfield, C., Olson, H., Alexander, C., 2005. Recent and modern marine erosion on the New Jersey outer shelf. *Mar. Geol.* 216, 275–296.
- Goy, J.L., Zazo, C., 1973. Estudio morfotectónico del Cuaternario en el Óvalo de Valencia. *Trabajos sobre Neógeno-Cuaternario. Actas I Reunión Nacional Grupo de Trabajo del Cuaternario*, Madrid 71–81.
- Goy, J.L., Zazo, C., 1988. Sequences of quaternary marine levels in Elche Basin (Eastern Betic Cordillera, Spain). *Palaeogeogr. Palaeoclimatol. Palaeoecol.* 68 (2/4), 301–310.
- Goy, J.L., Zazo, C., Dabrio, C.J., Lario, J., Borja, F., Sierro, F.J., Flores, J.A., 1996. Global and regional factors controlling changes of coastlines in southern Iberia (Spain) during the Holocene. *Quat. Sci. Rev.* 15, 773–780.
- Green, A.N., Smith, A.M., 2012. Can ancient shelf sand ridges be mistaken for Gilbert-type deltas? Examples from the Vryheid Formation, Ecca Group, KwaZulu-Natal, South Africa. *J. Afr. Earth Sci.* 76, 27–33.
- Harris, P.T., 1988. Sediments, bedforms and bedload transport pathways on the continental shelf adjacent to Torres Strait, Australia—Papua New Guinea. *Cont. Shelf Res.* 8 (8), 979–1003.
- Harrison, S.E., Locker, S.D., Hine, A.C., Edwards, J.H., Naar, D.F., Twichell, D.C., Mallinson, D.J., 2003. Sediment-starved sand ridges on the mixed carbonate/siliciclastic inner shelf of west-central Florida. *Mar. Geol.* 200, 171–194.
- Hoogendoorn, E.L., Dalrymple, R.W., 1986. Morphology, lateral migration, and internal structures of shoreface-connected ridges, Sable Island Bank, Nova Scotia, Canada. *Geology* 14, 400–403.
- Hernández-Molina, F.J., Somoza, L., Rey, J., Pomar, L., 1994. Late Pleistocene-Holocene sediments on the Spanish continental shelves: Model for very high resolution sequence stratigraphy. *Mar. Geol.* 120 (3–4), 129–174.
- Houboldt, J.J.H.C., 1968. Recent sediments in the southern bight of the North Sea. *Geol. Mijnb.* 47, 245–273.

- Houthuys, R., Trentesaux, A., Dewolf, P., 1994. Storm influences on a tidal sandbanks surface (Middelkerke Bank, southern North Sea). *Mar. Geol.* 121, 23–41.
- Hyne, N.J., Goodell, H.G., 1967. Origin of the sediments and submarine geomorphology of the inner continental shelf off Choctawhatchee Bay, Florida. *Mar. Geol.* 5, 299–313.
- Huthnance, J.M., 1982a. On one mechanism forming linear Sand banks. *Estuarine Coast Ma. Sci.* 14, 79–99.
- Huthnance, J.M., 1982b. On the formation of Sand banks of finite extent. *Estuarine Coast Mar Sci.* 14, 277–299.
- Ikehara, K., 1998. Sequence stratigraphy of tidal sand bodies in the Bungo Channel, southwest Japan. *Sediment. Geol.* 122, 233–244.
- Ikehara, K., Kinoshita, Y., 1994. Distribution and origin of subaqueous dunes on the shelf of Japan. *Mar. Geol.* 120, 75–87.
- ITGE, 1990. Mapa geológico de la plataforma continental española y zonas adyacentes. Escala 1:200.000 Murcia. Medialdea Vega, J. (dir) Instituto Tecnológico GeoMinero de España.
- ITGE, 1990. Mapa geológico de la plataforma continental española y zonas adyacentes. Escala 1:200.000 Elche-Alicante. González García, E. (dir) Instituto Tecnológico GeoMinero de España.
- Jordà, G., De Mey, P., 2010. Caracterización de la dinámica del error en un modelo 3D de la costa del mar catalán usando modelos estocásticos. *Cont. Shelf Res.* 30, 419–441.
- Jordi, A., Basterretxea, G., Wang, D.P., 2011. Local versus remote wind effects on the coastal circulation of a microtidal bay in the Mediterranean Sea. *J. Mar. Syst.* 88, 312–322.
- Kubicki, A., 2008. Large and very large subaqueous dunes on the continental shelf off southern Vietnam, South China Sea. *Geo-Mar. Lett.* 28, 229–238.
- Kuijpers, A., Werner, F., Rumohr, J., 1993. Sandwaves and other large-scale bedforms as indicators of non-tidal surge currents in the Skagerrak off northern Denmark. *Mar. Geol.* 111 (3–4), 209–221.
- Kenyon, N.H., Belderson, R.H., Stride, A.H., Johnson, M.A., 1981. Offshore tidal sandbanks as indicators of net sand transport and as potential deposits. *International Association of Sedimentologists, Special Publication* 5, 257–268.
- Li, M.Z., Amos, C.L., 1999. Sheet flow and large wave ripples under combined waves and currents: field observations, model predictions and effects on boundary layer dynamics. *Cont. Shelf Res.* 19 (5), 637–663.
- Lambeck, K., Bard, E., 2000. Sea-level change along the French Mediterranean coast since the time of the last Glacial Maximum. *Earth Planet. Sci. Lett.* 175 (3–4), 203–222.
- Lane, E.M., Restrepo, J.M., 2007. Shoreface-connected ridges under the action of waves and currents. *Journal of Fluid Mechanics* 582, 23–52.
- Li, M.Z., King, E.L., 2007. Multibeam bathymetric investigations of the morphology of sand ridges and associated bedforms and their relation to storm processes, Sable Island Bank. *Scott. Shelf. Mar. Geol.* 243 (1–4), 200–228.
- Liu, Z., Berné, S., Saito, Y., Yu, H., Trentesaux, A., Uehara, K., Yin, P., Liu, J.P., Li, C., Hu, G., Wang, X., 2007. Internal architecture and mobility of tidal sand ridges in the East China Sea. *Cont. Shelf Res.* 27 (13), 1820–1834.
- Lo Iacono, C., Guillen, J., Puig, P., Ribo, M., Ballesteros, M., Palanques, A., Farran, M., Acosta, J., 2010. Large-scale bedforms along a tideless outer shelf setting in the western Mediterranean. *Cont. Shelf Res.* 30 (17), 1802–1813.
- Lobo, F.J., Hernández-Molina, F.J., Somoza, L., Rodero, J., Maldonado, A., Barnolas, A., 2000. Patterns of bottom current flow deduced from dune asymmetries over the Gulf of Cadiz shelf (southwest Spain). *Mar. Geol.* 164 (3–4), 91–117.
- Maillard, A., Mauffret, A., 2012. Structure and present-day compression in the offshore area between Alicante and Ibiza Island (Eastern Iberian Margin). *Tectonophysics* 591, 116–130.
- Maldonado, A., Zamarreño, I., 1983. Modelos sedimentarios en las plataformas continentales del Mediterráneo español: factores de control, facies y procesos que rigen su desarrollo. In: Castellví, J. (Ed.), *Estudio oceanográfico de la plataforma continental*. Sem Interdisc Hispanic-American Cooperative Research Project. Gráficas Buper, Barcelona, pp. 25–83.
- Maldonado, A., Swift, D., Young, R., Han, G., Nittrouer, C., DeMaster, D., Rey, J., Palomo, C., Acosta, J., Ballester, A., Castellví, J., 1983. Sedimentation on the Valencia continental shelf: preliminary results. *Cont. Shelf Res.* 2 (2/3), 125–142.
- Marco-Barbas, J., 2010. *Ecología y geoquímica de ostrácodos como indicadores paleoambientales en ambientes marginales marinos: Un ejemplo de estudio. (PhD Thesis) La Albufera de Valencia*. University of Valencia, Valencia 300.
- McBride, R.A., Moslow, T.F., 1991. Origin, evolution, and distribution of shoreface sand ridges, Atlantic inner shelf, USA. *Mar. Geol.* 97, 57–85.
- McClenen, C.E., McMaster, R.L., 1971. Probable Holocene transgressive effects on the geomorphic features of the continental shelf off New Jersey, United States. *Maritime Sediments* 7, 69–72.
- Muñoz, A., Lastras, G., Ballesteros, M., Canals, M., Acosta, J., Uchupi, E., 2005. Sea floor morphology of the Ebro Shelf in the region of the Columbretes Islands, Western Mediterranean. *Geomorphology* 72, 1–18.

- Olaiz, A.J., Muñoz-Martín, A., De Vicente, G., Vegas, R., Cloetingh, S., 2009. *Tectonophysics* 474, 33–40 (Topo-Europe: Special Issue).
- Park, S.C., Han, H.S., Yoo, D.G., 2003. Transgressive sand ridges on the mid-shelf of the southern sea of Korea (Korea Strait): formation and development in high-energy environments. *Mar. Geol.* 193, 1–18.
- Parker, G., Lanfredi, N.W., Swift, D.J.P., 1982. Seafloor response to flow in a southern hemisphere sand ridge field: Argentine inner shelf. *Mar. Geol.* 33, 195–216.
- Piper, D.J.W., 1991. Seabed geology of the Canadian eastern continental-shelf. *Cont. Shelf Res.* 11 (8–10), 1013–1035.
- Ramsay, P.J., Smith, A.M., Mason, T.R., 1996. Geostrophic sand ridge, dune fields and associated bedforms from the northern KwaZulu-Natal shelf, south-east Africa. *Sedimentology* 43, 407–419.
- Renault, J.P., Boillot, G., Mauffret, A., 1984. The Western Mediterranean Basin geological evolution. *Mar. Geol.* 55 (3–4), 447–477.
- Rey, J., Díaz Del Río, V., 1982. Sand ridges in the west Mediterranean Continental Shelf (Valencia, Spain), morphology and seismic character. *Rapp. P.-V. Comm. Int. Mer. Mediterr.* 28, 261–262.
- Rey, J., Díaz del Río, V., 1983. Aspectos geológicos sobre la estructura poco profunda de la plataforma del Levante Español. In: Castellví, J. (Ed.), *Estudio oceanográfico de la plataforma continental*. Seminario Científico Interdisciplinaria, Cádiz. Gráficas Buper, Barcelona, pp. 53–74.
- Rey, J., Díaz del Río, V., 1984. Algunos aspectos morfoestructurales del Cuaternario submarino en la plataforma continental del Mediterráneo Español. *Thalassa* 2 (1), 23–29.
- Rey, J., Fumanal, P., 1996. The Valencian coast (Western Mediterranean): neotectonics and geomorphology. *Quat. Sci. Rev.* 15 (8/9), 789–802.
- Rey, J., Medialdea, T., 1989. Los sedimentos cuaternarios superficiales del margen continental español. *Inst. Esp. Oceanogr. Publ. Espec.* 3.
- Rey, J., Fernández, L.M., Blázquez, A.M., 1999. Identificación de las unidades morfosedimentarias cuaternarias en la plataforma interna del litoral del País Valenciano: el rol de los factores morfoestructurales y eustáticos. In: Fumanal, P. (Ed.), *Geoarqueología i Quaternari litoral*. Memorial María Pilar Fumanal. Universitat de València, València, pp. 403–418.
- Rine, J.M., Tillman, R.W., Culver, S.J., Swift, D.J.P., 1991. Generation of late Holocene sand ridges on the middle continental shelf of New Jersey, USA — evidence of formation in a mid-shelf setting based on comparisons with a nearshore ridge. *Int. Assoc. Sedimentol. Spec. Publ.* 14, 395–423.
- Rueda, J., Mezcuá, J., 2005. Near-real-time seismic moment-tensor determination in Spain. *Seismol. Res. Lett.* 76, 455–465.
- Sanjaume, E., Carmona, P., 1995. L'Albufera de València: rasgo geomorfológicos y evolución cuaternaria. *El Cuaternario del País Valenciano*. Universidad de Valencia- AEQUA, Valencia, pp. 155–161.
- Silva, P.G., Goy, J.L., Zazo, C., Bardají, T., 2003. Fault-generated mountain fronts in southeast Spain: geomorphologic assessment of tectonic and seismic activity. *Geomorphology* 50, 203–225.
- Snedden, J.W., Dalrymple, R.W., 1999. Modern shelf sand ridges: from historical perspective to a unified hydrodynamic and evolutionary model. In: Bergman, K.M., Snedden, J.W. (Eds.), *Isolated Shallow Marine Sand Bodies*. Sequence Stratigraphic Analysis and Sedimentologic Interpretation: SEPM, Special Publication, 64, pp. 13–28.
- Snedden, J.W., Tillman, R.W., Kreisa, R.D., Schweller, W.J., Culver, S.J., Winn, R.D., 1994. Stratigraphy and genesis of a modern shoreface-attached sand ridge, Peahala ridge, New Jersey. *J. Sediment. Res.* 64, 560–581.
- Snedden, J.W., Tillman, R.W., Culver, S.J., 2011. Genesis and evolution of a mid-shelf, storm-built sand ridge, New Jersey continental shelf, USA. *J. Sediment. Res.* 81 (7–8), 534–552.
- Somoza, L., Barnolas, A., Arasa, A., Maestro, A., Rees, J.G., Hernandez-Molina, F.J., 1998. Architectural stacking patterns of the Ebro delta controlled by Holocene high-frequency eustatic fluctuations, delta-lobe switching and subsidence processes. *Sediment. Geol.* 117 (1–2), 11–32.
- Stocchi, P., Spada, G., 2009. Influence of glacial isostatic adjustment upon current sea level variations in the Mediterranean. *Tectonophysics* 474, 56–68.
- Stubblefield, W.L., Swift, D.J.P., 1981. Grain size variation across sand ridges. New Jersey continental shelf. *Geo-Mar. Lett.* 1 (1), 45–48.
- Swift, D.J.P., Field, M.E., 1981. Evolution of a classic sand ridge field: Maryland sector, North American inner shelf. *Sedimentology* 28, 461–482.
- Stubblefield, W.L., McGrail, D.W., Kersey, D.G., 1984. Recognition of transgressive and post-transgressive sand ridges on the New Jersey Continental shelf. In: Tillman, R.W., Siemens, C.T. (Eds.), *Siliciclastic Shelf Sediments*. SEPM Special Pub, 34, pp. 1–24.

- Swift, D.J.P., Parker, G., Lanfredi, M.W., Perillo, G., Figge, K., 1978. Shoreface-connected sand ridges on American and European shelves: a comparison. *Estuar. Coast. Mar. Sci.* 7, 257–273.
- Swift, D.J.P., McKinney, T.F., Stahl, L., 1984. Recognition of transgressive and posttransgressive sand ridges on the New Jersey continental shelf: discussion. In: Tillman, R.W., Siemers, C.T. (Eds.), *Siliciclastic Shelf Sediments*. Soc. Econ. Paleontologists and Mineralogists, Tulsa, pp. 25–36.
- Trentesaux, A., Stolk, A., Tessier, B., Chamley, H., 1994. Surficial sedimentology of the Middelkerke Bank (Southern North Sea). *Mar. Geol.* 121, 43–55.
- Trentesaux, A., Stolk, A., Berné, S., 1999. Sedimentology and stratigraphy of a tidal sand bank in the southern North Sea. *Mar. Geol.* 159, 253–272.
- Trowbridge, J.H., 1995. A mechanism for the formation and maintenance of shore-oblique sand ridges on storm-dominated shelves. *J. Geophys. Res.* 100, 16071–16086.
- Twicheil, D.C., Brooks, G., Gelfenbaum, G., Paskevich, V., Donahue, B., 2003. Sand ridges off Sarasota, Florida: a complex facies boundary on a low-energy inner shelf environment. *Mar. Geol.* 200 (1–4), 243–262.
- Van de Meene, J.W.H., Van Rijn, L.C., 2000. The shoreface-connected ridges along the central Dutch coast — part I: field observations. *Cont. Shelf Res.* 20, 2295–2323.
- Van de Meene, J.W.H., Boersma, J.R., Terwindt, J.H.J., 1996. Sedimentary structures of combined low deposits from the shoreface-connected ridges along the central Dutch coast. *Mar. Geol.* 131, 151–175.
- Viñals, M.J., 1995. Secuencia estratigráfica y evolución morfológica del extremo meridional del Golfo de Valencia. In: Fumanal, M.P., Bernabeu, J. (Eds.), *El Cuaternario del País Valenciano*. Universidad de València, València, pp. 163–167.
- Viñals, M.J., Fumanal, M.P., 1995. Quaternary development and evolution of the sedimentary environments in the Central Mediterranean Spanish coast. *Quat. Int.* 29/30, 119–128.
- Viñals, M.P., Belluomini, G., Fumanal, M.P., Dupré, M., Usera, J., Mestres, J., 1993. Rasgos paleoambientales holocenos de la Bahía de Xabia (Alicante). In: Fumanal, M.P., Bernabeu, J. (Eds.), *Estudios sobre Cuaternario. Medios Sedimentarios, Cambios Ambientales, Hábitat Humano*. Universidad de Valencia, Valencia, pp. 107–114.
- Wagle, B.G., Veerayya, M., 1996. Submerged sand ridges on the western continental shelf off Bombay, India: evidence for Late Pleistocene–Holocene sea-level changes. *Mar. Geol.* 136, 79–95.
- Walgreen, M., Calvete, D., de Swart, H.E., 2002. Growth of large-scale bed forms due to storm-driven and tidal currents: a model approach. *Cont. Shelf Res.* 22, 2777–2793.
- Wang, Y., Zhang, Y., Zou, X., Zhu, D., Piper, D., 2012. The sand ridge field of the South Yellow Sea: origin by river–sea interaction. *Mar. Geol.* 291–294, 132–146.
- Whitmeyer, S.J., FitzGerald, D.M., 2008. Episodic dynamics of a sand wave field. *Mar. Geol.* 252, 24–37.
- Yang, C.S., 1989. Active, moribund and buried tidal sand ridges in the East China Sea and the southern Yellow Sea. *Mar. Geol.* 88 (1–2), 97–116.
- Yoo, D.G., Lee, C.W., Kim, S.P., Jin, J.H., Kim, J.K., Han, H.C., 2002. Late Quaternary transgressive and highstand systems tracts in the northern East China Seamount-shelf. *Mar. Geol.* 187, 313–328.
- Young, R.A., Swift, D.J.P., Nittrouer, C.A., Demaster, D.J., Bergenback, B., 1983. Event-dominated sediment transport on the Valencian continental shelf, Spain, and its effect on sediment accumulation and Holocene stratigraphy. In: Castellví, J. (Ed.), *Estudio oceanográfico de la plataforma continental Española*. Sem Interdisc Hispanic- American Cooperative Research Project. Gráficas Buper, Barcelona, pp. 1–13.
- Zazo, C., Goy, J.L., Dabrio, C.J., Bardaji, T., Somoza, L., Silva, P.G., 1993. The last interglacial in the Mediterranean as a model for the present interglacial. *Glob. Planet. Chang.* 7 (1/3), 109–117.

Figure captions

Fig. 1. Location of the study area (black framed area), and location of the buoys employed to determine the oceanographic setting.

Fig. 2. Earthquake representation (source: database from 1258 to 2013 — Instituto Geográfico Nacional) based on magnitude (MbLg) and depth (km) of the events. Regional focal mechanism of the area. Histogram representing the frequency of each magnitude range.

Fig. 3. A. Storm wave diagram (data source: point WANA2083111, from the Puertos del Estado database, Spain). B. Current diagram (data source: Buoy II — 2630, from the Puertos del Estado database, Spain).

Fig. 4. Location of the data acquired during the geophysical and sedimentological surveys: multibeam mapping, seismic data and sediment samples.

Fig. 5. DEM representing multibeam data; mapping of the sand waves morphologies identified. D18, D20, D21 and D22 have been delimited with seismic data..

Fig. 6. Morphological characterizations of the sand waves: (A) DEM with the shelf morphologies identified as well as the position of topographic profiles; (B) slope map with graduated color scale; (C) topographic profiles from NW to SE..

Fig. 7. Heights (h) versus wavelengths (λ) of the sand ridges: study area (blue dots), length/height relationships proposed by Flemming (1988), trend of the global mean equation by Flemming (1988) (gray line). Regression curves for the Columbretes bedforms (red line) (Lo Iacono et al., 2009) and of similar bedforms formed in microtidal shelves of many continental margins around the world (green line) (Gardner et al., 2005, Gardner et al., 2007, Ikehara, 1998, Kubicki, 2008, Li and King, 2007).

Fig. 8. Sediment sample of C4 station, water depth at – 80 m (Position in Fig. 4): (A) triangle GRADISTAT (Blott and Pye, 2001), (B) superficial representation of gravel, sand, silt and mud, and (C) photograph of 9, 12 and 20 cm with cobbles and pebbles

Fig. 9. 3D mapping, with 2 sections of the high resolution profile recorded in the Gulf of Valencia (GeoPulse). Two parallel profiles 1350 m apart, NNE–SSW. Symbols: FRW = forced regressive wedge (FRW1, FRW2); St = transgressive subsystems; P = progradation downlap; A = aggradational unit; T = transgressive surface. Location profile, see Fig. 4.

Fig. 10. 3D mapping, with 4 high resolution profiles recorded in the Gulf of Valencia (TOPAS). N–S Orientation profile 1: 60 m in depth; profile 2: 70 m; profile 3: 75 m and profile 4: 80 m. Symbols: SU = sand waves; RS = ravinement surface; St2 = transgressive subsystem; A2 = aggradational stage; and T2 = transgressive stage. Location profile, see Fig. 4.

Fig. 11. Historic profile (Line L-6-7-8-GC 83-1-3.5 kHz) from the south part of the study area W–E. Symbols: PB = paleo-barrier (Tyrrhenian); SU = sand waves unit; RS = ravinement surface; T2 = transgressive surface; and SLU = slump unit. Location profile, see Fig. 4.

Fig. 12. High resolution seismic profile W–E on the continental shelf in the Gulf of Valencia (position in Fig. 2). Symbols: SU = sand waves unit; RS = ravinement surface; A2 = aggradational. Location profile, see Fig. 4.

Fig. 13. Regional relative sea level curve in the Gulf of Valencia for a 0.3 mm/y rate of subsidence for the last 22 ky BP. Sea level curve modified from Bassetti et al. (2006).

Fig. 14. Mechanism of formation of the sand waves according to the present depth below sea level (m). Two storm events (extreme storm $H_s = 5$ m, $T_p = 11$ s; normal storms: $H_s = 2$ m, $T_p = 8$ s).

Table 1. Significant parameters for all bedforms (mound and dunes): All values are given in meters. d Min, minor water depth; d Max, major water depth; L, length; W Min, minor horizontal extension; W Max, major horizontal extension; W, average horizontal extension; H, height; L/H, symmetry index.

Figure 1

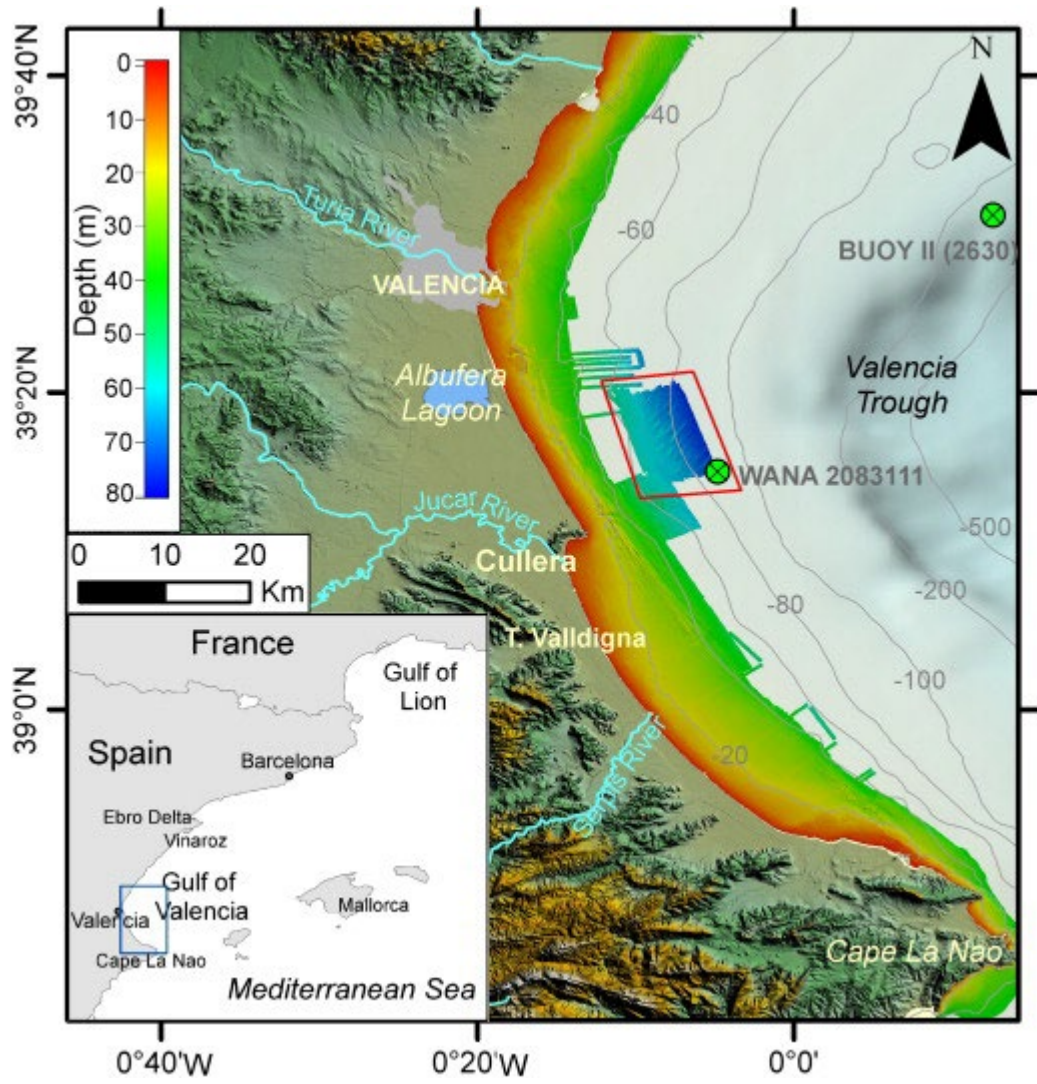


Figure 2

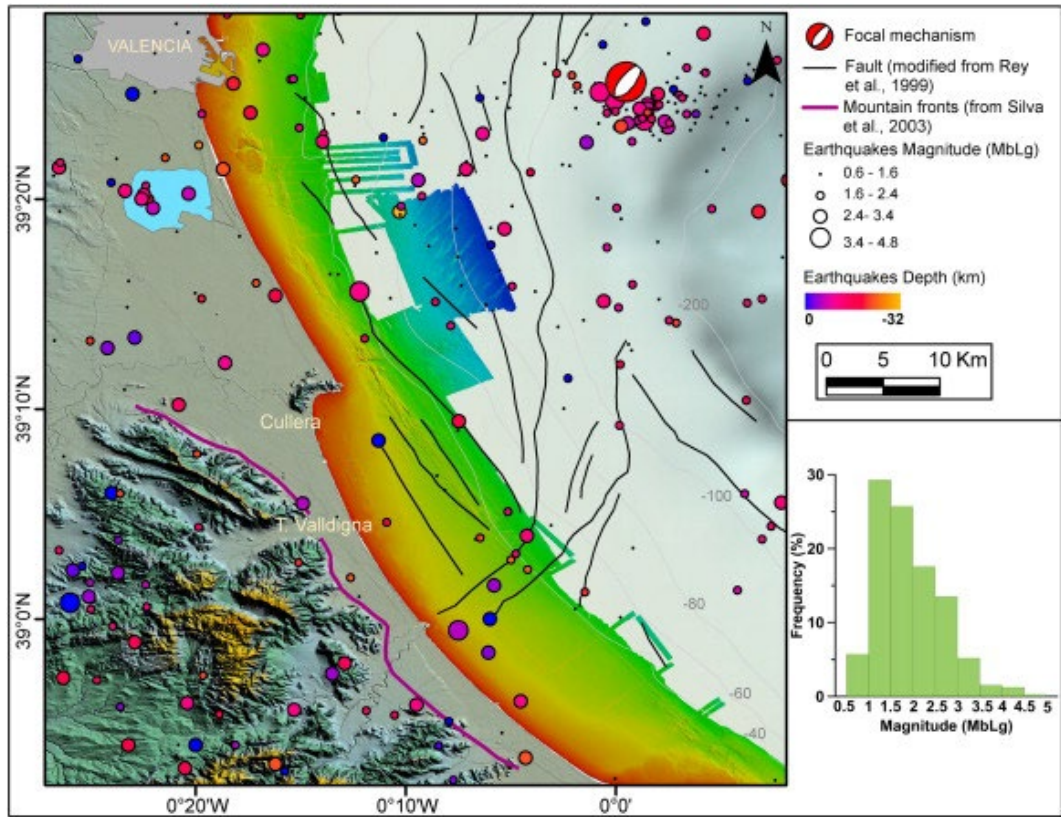


Figure 3

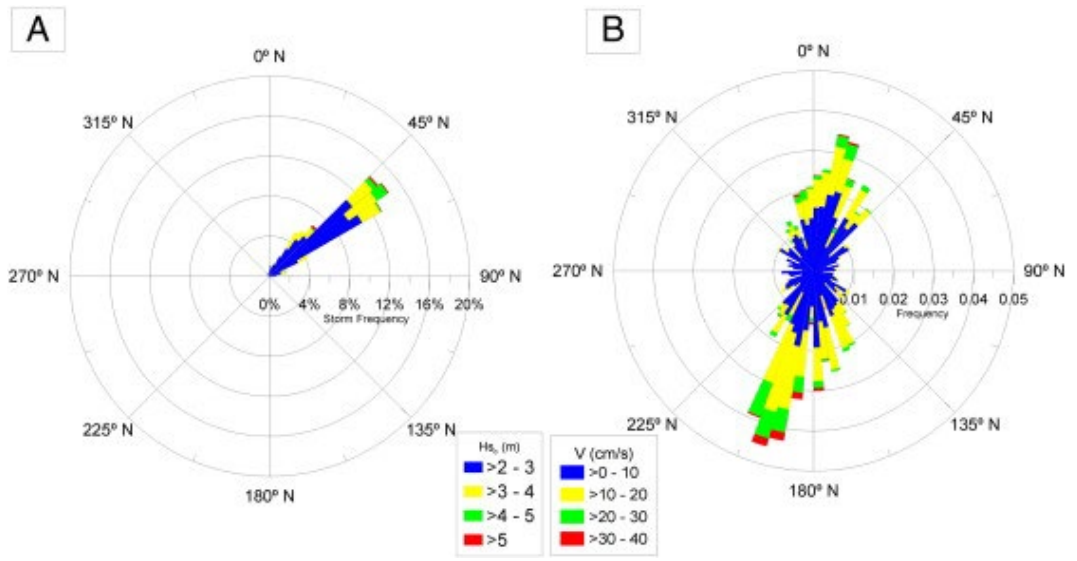


Figure 4

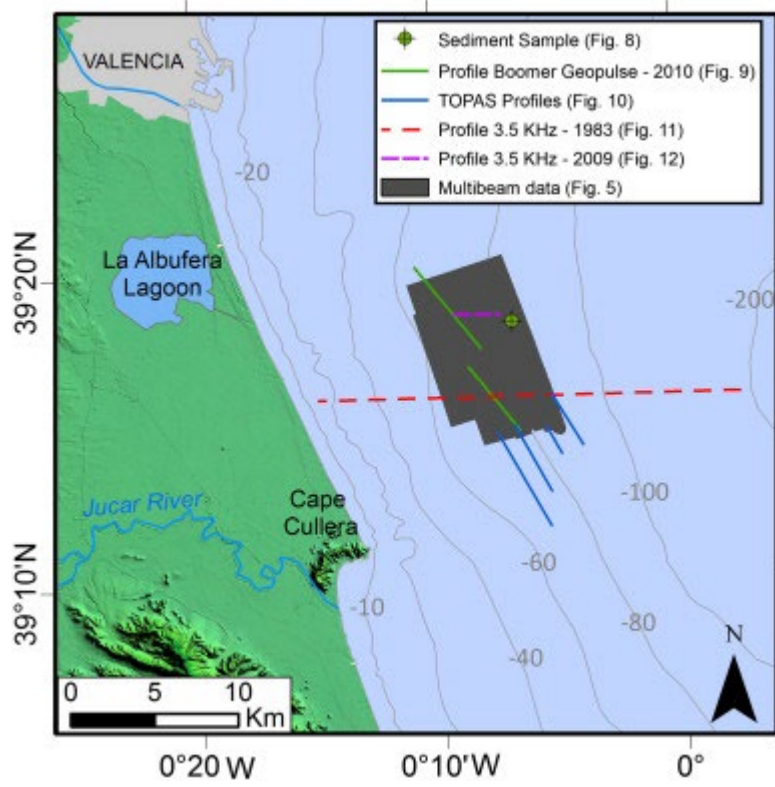


Figure 5

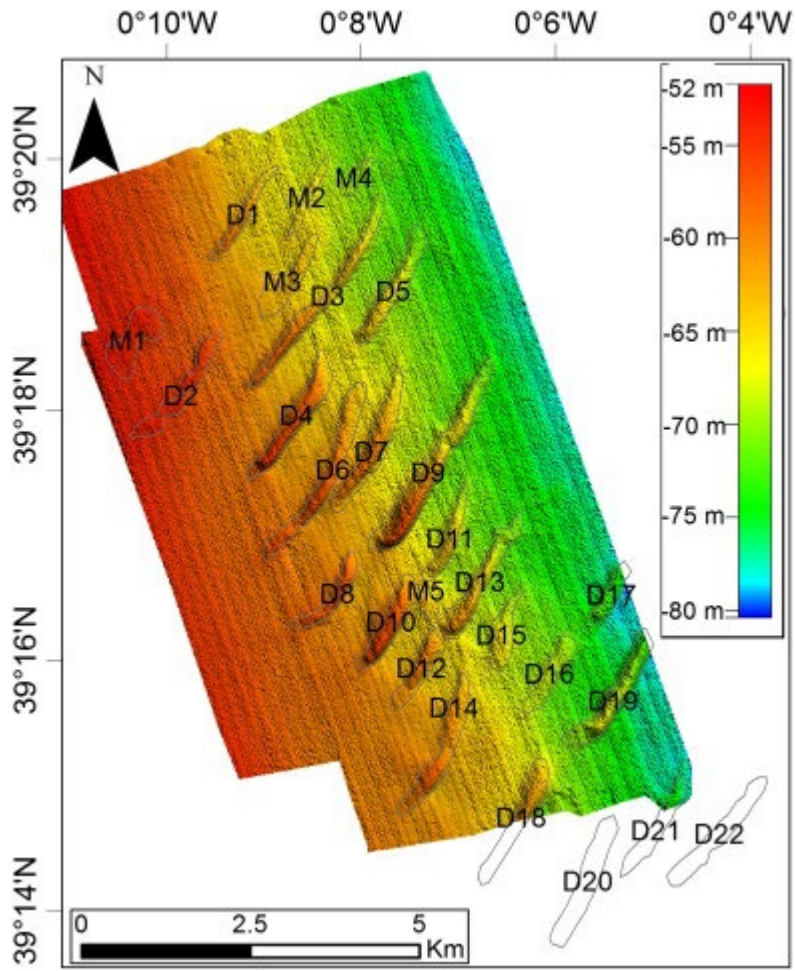


Figure 6

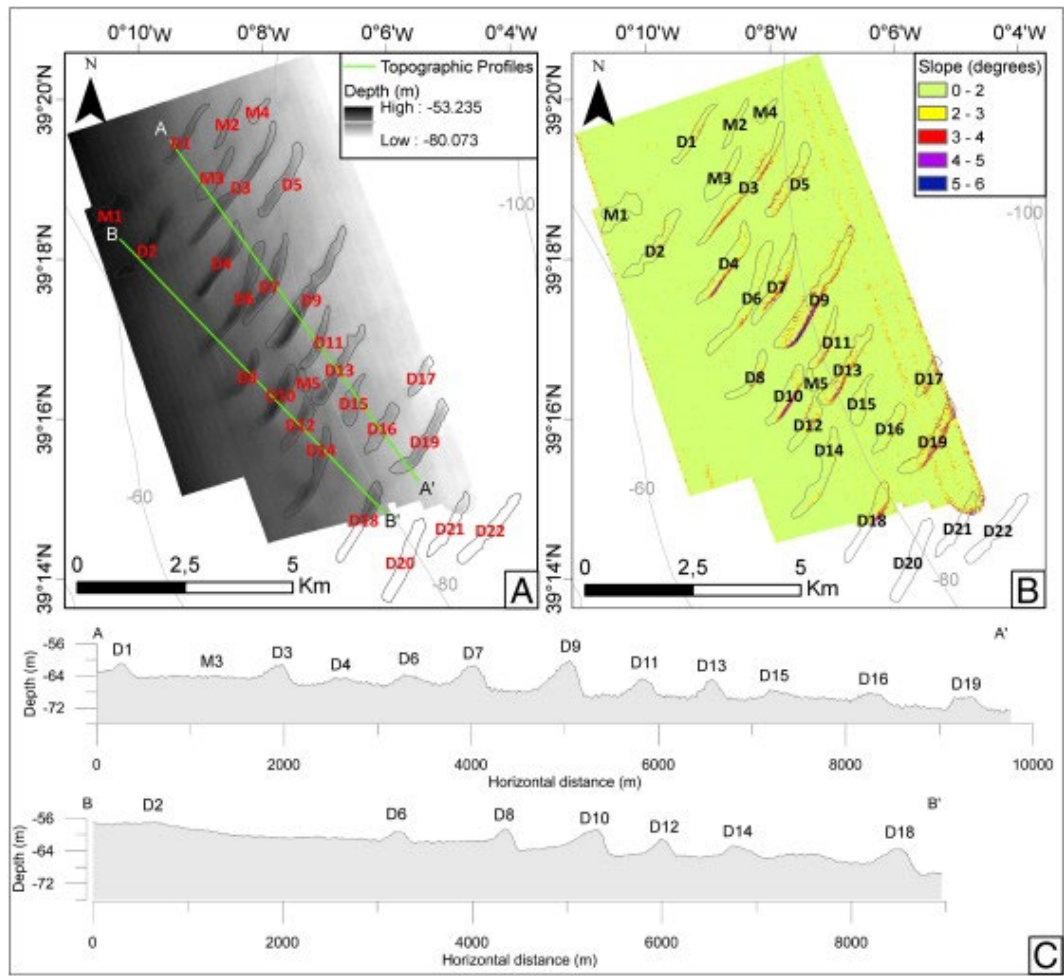


Figure 7

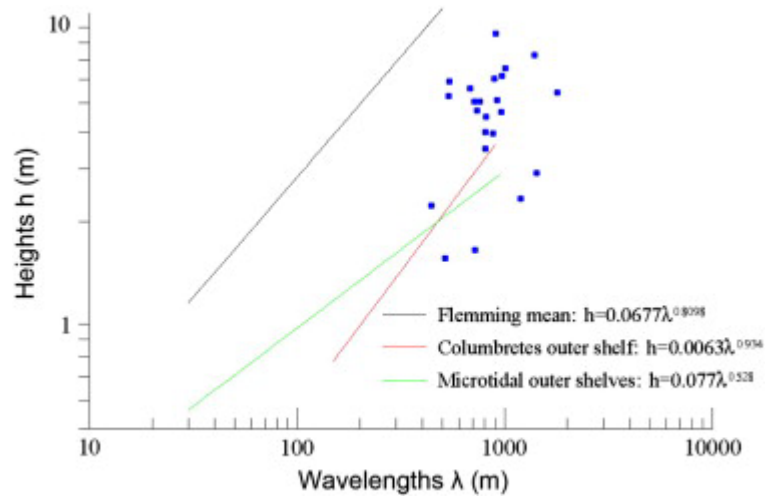


Figure 8

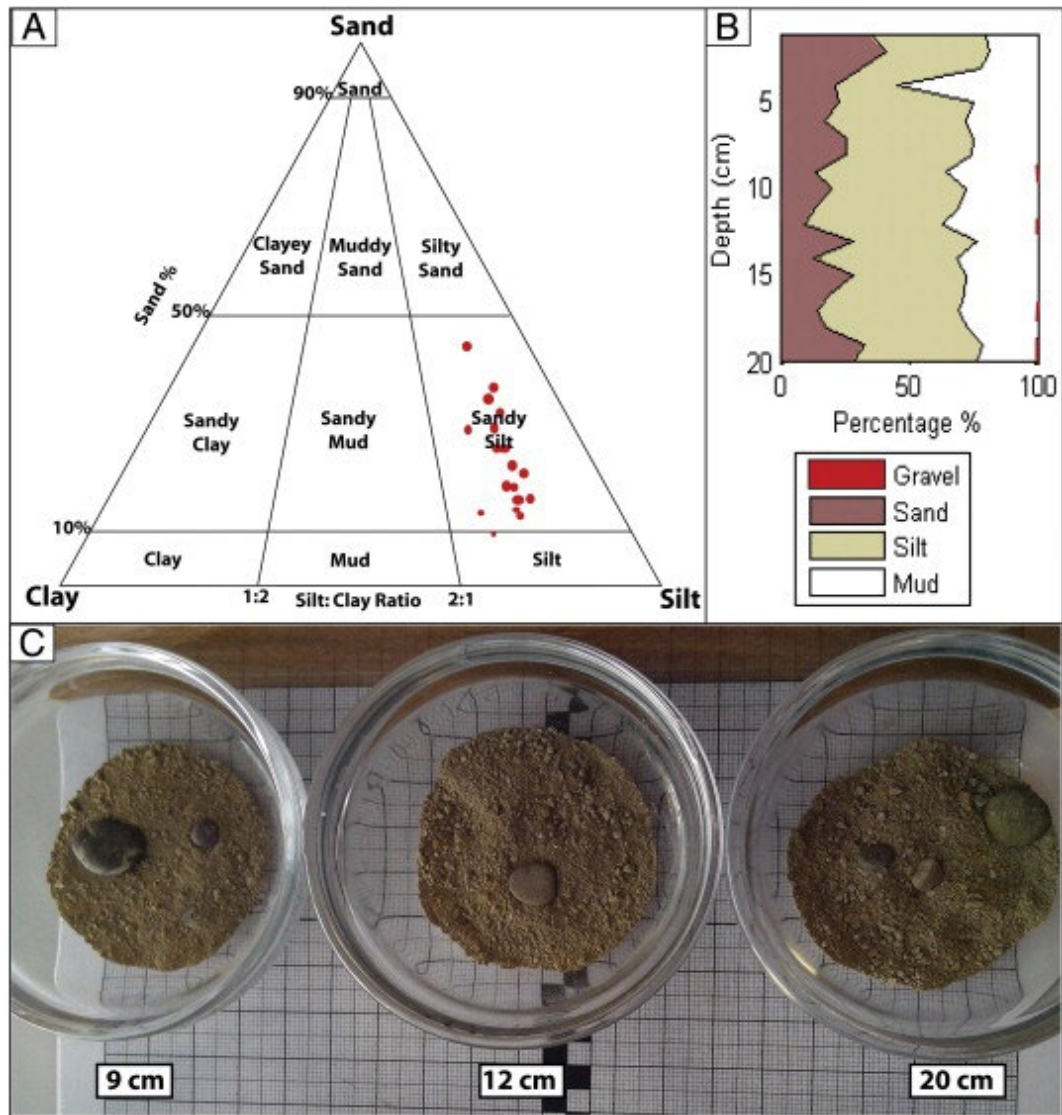


Figure 9

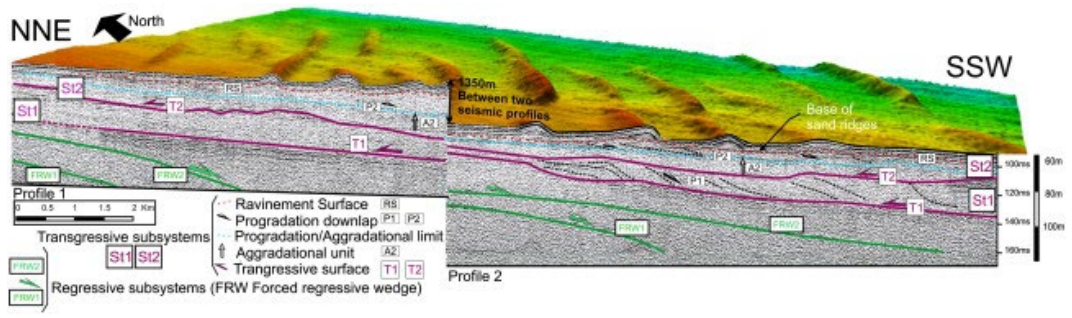


Figure 10

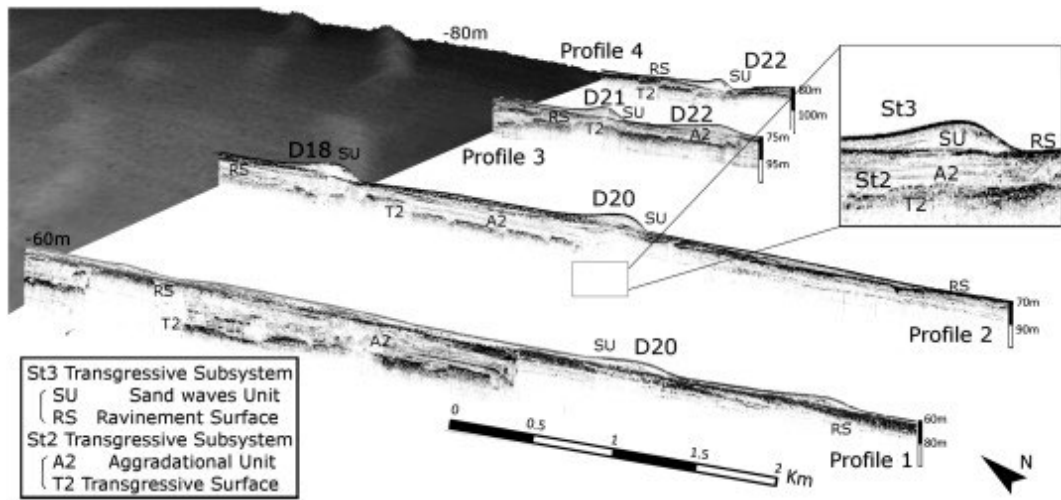


Figure 11

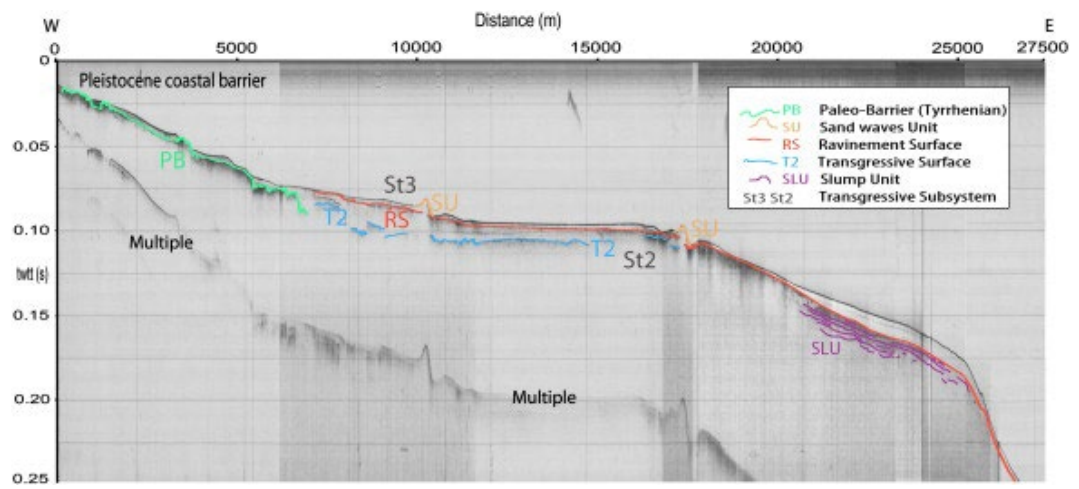


Figure 12

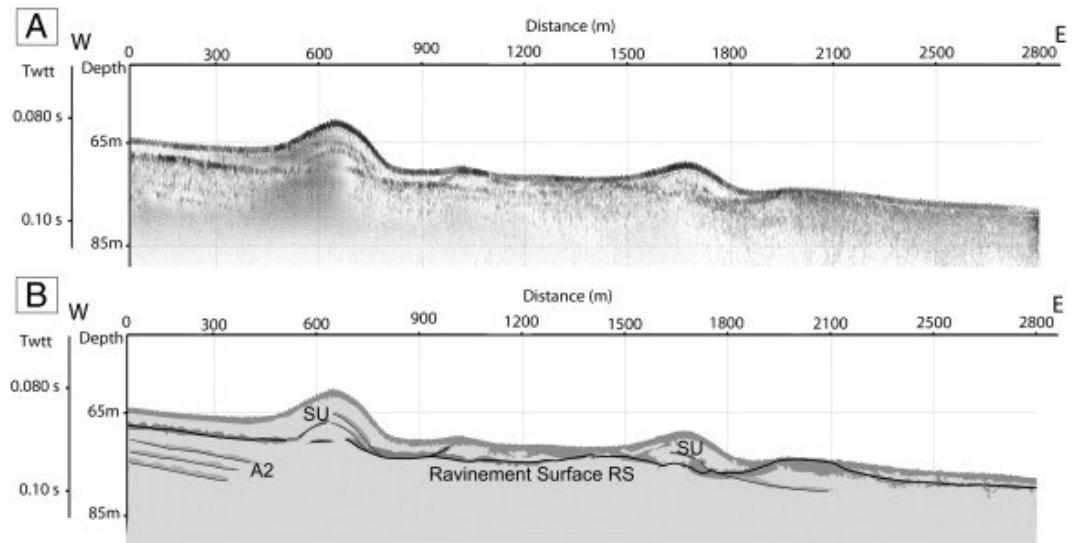


Figure 13

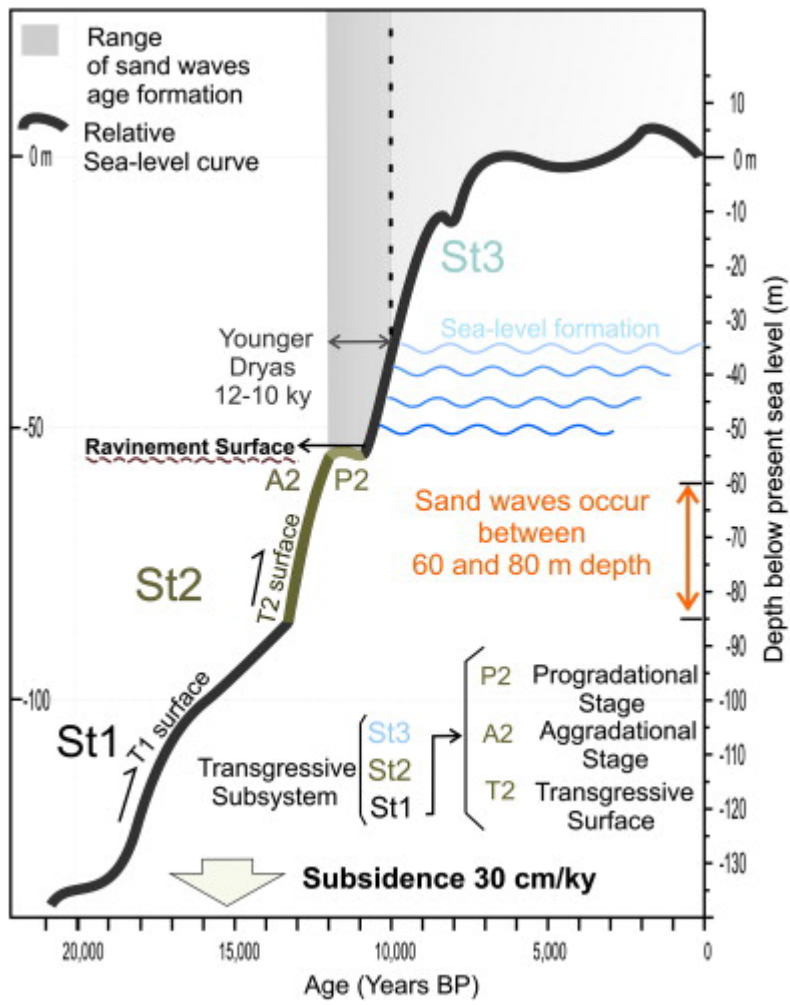


Figure 14

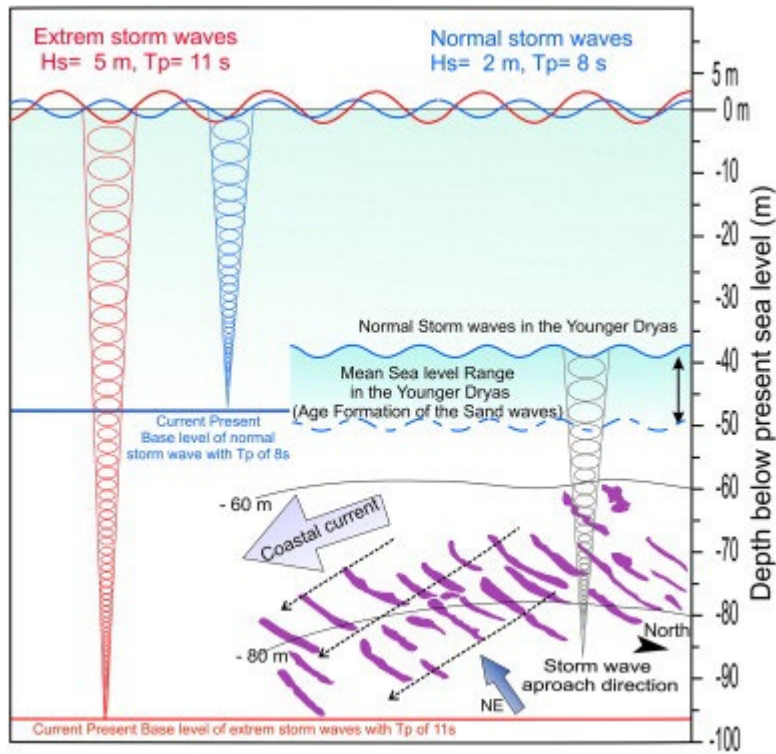


Table 1

| | Area | d Min | d Max | L | W Min | W Max | H | L/H |
|----|---------|-------|-------|------|-------|-------|------|------|
| M1 | 418,202 | -56 | -57 | 992 | 220 | 580 | 1.87 | 5.30 |
| M2 | 143,540 | -65 | -68 | 1442 | 100 | 148 | 1.6 | 9.01 |
| M3 | 362,137 | -64 | -66 | 955 | 176 | 455 | 2.26 | 4.22 |
| M4 | 110,618 | -68 | -70 | 698 | 116 | 212 | 1.5 | 4.65 |
| M5 | 111,787 | -64 | -65 | 550 | 127 | 285 | 2 | 2.75 |

| Total values of mounts | Area | Depth | L | W | H |
|------------------------|-----------|-------|------|-----|-------|
| Average | 229,256.8 | -64 | 927 | 162 | 1.846 |
| Minimum | 110,618 | -63 | 550 | 147 | 1.5 |
| Maximum | 418,202 | -65 | 1442 | 178 | 2.26 |

| | Area | d Min | d Max | L | W Min | W Max | H | L/H |
|-----|---------|-------|-------|------|-------|-------|------|------|
| D1 | 225,536 | -61 | -66 | 1575 | 110 | 193 | 5.05 | 3.11 |
| D2 | 413,377 | -57 | -60 | 1366 | 143 | 261 | 3.96 | 3.44 |
| D3 | 530,744 | -60 | -71 | 3404 | 113 | 253 | 5.29 | 6.43 |
| D4 | 538,029 | -58 | -65 | 1727 | 196 | 380 | 6.02 | 2.86 |
| D5 | 453,870 | -64 | -71 | 2129 | 210 | 289 | 3.99 | 5.33 |
| D6 | 665,765 | -58 | -64 | 2580 | 192 | 294 | 4.68 | 5.51 |
| D7 | 550,805 | -60 | -67 | 2406 | 157 | 346 | 5.92 | 4.06 |
| D8 | 255,188 | -58 | -62 | 1265 | 190 | 205 | 2.38 | 5.31 |
| D9 | 894,610 | -59 | -72 | 3085 | 160 | 400 | 8.54 | 3.61 |
| D10 | 430,725 | -58 | -63 | 1311 | 234 | 312 | 6.17 | 2.12 |
| D11 | 252,016 | -64 | -70 | 1573 | 124 | 229 | 5.06 | 3.10 |
| D12 | 329,819 | -62 | -64 | 880 | 240 | 319 | 4.71 | 1.86 |
| D13 | 498,824 | -62 | -73 | 2090 | 184 | 361 | 5.61 | 3.72 |
| D14 | 588,192 | -60 | -65 | 2080 | 233 | 420 | 5.1 | 4.07 |
| D15 | 292,619 | -66 | -70 | 1331 | 130 | 330 | 3.5 | 3.80 |
| D16 | 327,285 | -68 | -71 | 800 | 214 | 312 | 4.5 | 1.77 |
| D17 | 203,769 | -71 | -77 | 723 | 201 | 310 | 5.43 | 1.33 |
| D18 | 462,411 | -60 | -66 | 2091 | 294 | 295 | 7.26 | 1.33 |
| D19 | 522,584 | -67 | -74 | 1336 | 238 | 300 | 6.55 | 2.03 |
| D20 | 580,004 | -60 | -76 | 2104 | 176 | 176 | 2.91 | 7.23 |
| D21 | 346,373 | -68 | -76 | 1757 | 214 | 265 | - | - |
| D22 | 485,200 | -69 | -77 | 2135 | 248 | 248 | - | - |

| Total values of dunes | Area | Depth | L | W | H |
|-----------------------|---------|-------|------|-------|------|
| Average | 447,624 | 69.1 | 1806 | 227.1 | 5.13 |
| Minimum | 203,769 | 62.3 | 723 | 192 | 2.38 |
| Maximum | 894,610 | 69.1 | 3404 | 295.4 | 8.54 |